CHMP3 complex resides on MVB/late endosomes, but the localization of AMSH does not significantly correlate with its binding of CHMP3, even though aberrant endosomes are induced upon AMSH$^{dN3}$ expression.

### *Ubiquitinated cargo clearance requires both the CHMP3-binding capability and the DUB activity of AMSH*

We next investigated whether the CHMP3-binding capability of AMSH was important for AMSH's roles in vesicular traffic. For comparison, we prepared an enzymatically inactive AMSH, AMSH$^{E280A}$, basing our construct design on a report in which replacement of a glutamic acid residue (E20) by alanine within the JAMM motif of the *Archaeoglobus fulgidus* AfJAMM protein completely abolished the catalytic activity (Ambroggio *et al.*, 2004). To verify that the AMSH$^{E280A}$ mutant possessed no DUB activity, we performed an *in vitro* deubiquitination assay. As previously reported, wild-type AMSH showed no DUB activity for K48-linked ubiquitin chains (Fig. 3A, left panel), while it clearly cleaved ubiquitins from the K63-linked chains ($Ub_{2-7}$) (Fig. 3A, middle panel). Recombinant AMSH$^{E280A}$ produced no monomeric ubiquitins from the K48- or K63-linked ubiquitin chains. We also examined AMSH truncation mutants for their DUB activities. Two N-terminal deletion mutants, AMSH$^{dN2}$ and AMSH$^{dN3}$, showed catalytic activity similar to wild-type AMSH. These results show that AMSH carries a K63-linked ubiquitin-specific DUB activity, which is abrogated by the E280A mutation but is not affected by the deletion of the CHMP3-binding region.

To examine the effect of the CHMP3-binding capability and DUB activity of AMSH on ubiquitinated cargos *in vivo*, intracellular ubiquitin was immunostained following the transient introduction of AMSH, AMSH$^{E280A}$, or AMSH$^{dN3}$. For this experiment, we used the FK2 antibody, which specifically detects ubiquitin moieties on cargo proteins (Fujimuro *et al.*, 1994). When wild-type AMSH was expressed, only a marginal amount of ubiquitinated cargo was observed (Fig. 3B, top panels, arrowhead). Surprisingly, the transfection of AMSH$^{E280A}$ induced heavy staining of ubiquitinated cargo proteins, which merged with LAMP2 staining (Fig. 3B, middle panels, arrowheads). Deposits of FK2-positive cargo were also seen in EEA1-positive puncta (data not shown). Unexpectedly, the introduction of AMSH$^{dN3}$ also resulted in the marked deposition of ubiquitinated cargo on late endosomes, similar to that seen with AMSH$^{E280A}$ (Fig. 3B, bottom panels, arrowheads). These results suggest that not only the DUB activity of AMSH but also its CHMP3-binding capability is required for the normal clearance of ubiquitinated cargo from endosomes.

### *AMSH associates with the ESCRT-III complex, and its catalytic activity is not essential for the dissociation of the ESCRT-III complex*

Next, we asked whether AMSH is included in the ESCRT-III complex. Previous reports suggest that ESCRT-III is further divided into two subcomplexes, and the one that contains CHMP3 also includes CHMP2A or CHMP2B (Bowers *et al.*, 2004; Morita and Sundquist, 2004). By transient expression experiments using 293T cells, we found a physical interaction between CHMP2A and CHMP3, as well as CHMP2B and CHMP3 (Fig. 4A, lanes 7 and 8). The co-introduction AMSH induced the formation of ternary complexes, including AMSH, CHMP2A, and CHMP3, and AMSH, CHMP2B, and CHMP3 (Fig. 4A, lanes 5 and 6). We also observed that CHMP2A but not CHMP2B showed a weak association with AMSH, even in the absence of CHMP3 (Fig. 4A, lanes 3 and 4). These results suggest that AMSH is included in ESCRT-III, at least in a CHMP3-containing subcomplex.

Next, we set out to clarify whether AMSH is involved in MVB sorting. A characteristic property of class E VPS pathway is that they are often relocalized to aberrant endosomes induced by expression of catalytically inactive VPS4 mutant. We co-expressed GFP-AMSH and DsRed-Vps4$^{E228Q}$ and found that GFP-AMSH accumulated on aberrant DsRed-Vps4$^{E228Q}$-induced endosomes (Fig. 4B). Therefore, it is likely that AMSH is related to some MVB function.

We then wondered whether AMSH is essential for the association-disassociation of ESCRT-III, since the ESCRT-III complex in yeast is transiently formed on vesicular membranes and then subjected to constant dissociation by the ATPase activity of VPS4p (Babst *et al.*, 1998). We fractionated 293T cell lysates into their cytoplasmic and membrane components. In mock-transfected 293T cells, native CHMP3 localized to the cytoplasmic but not the membrane fraction, which included the LAMP1-positive late endosomes (Fig. 4C). Transient introduction of FLAG-tagged AMSH did not alter the localization of CHMP3. Likewise, the cytoplasmic localization of CHMP3 was unchanged by the introduction of AMSH$^{E280A}$ or VPS4. In sharp contrast, VPS4$^{E228Q}$, a dominant-negative mutant, induced CHMP3 localization to the membrane fraction. Because the overexpression of neither wild-type AMSH nor catalytically inactive AMSH altered the location of ESCRT-III relative to the membrane fraction, these results suggest that AMSH may not be essential for the proper functioning of the ESCRT-III association-dissociation machinery.

### *AMSH deubiquitinates cargo proteins before their lysosomal degradation and AMSH depletion induces endosomes stuffed with ubiquitinated cargo*

To further elucidate the roles played by AMSH at the

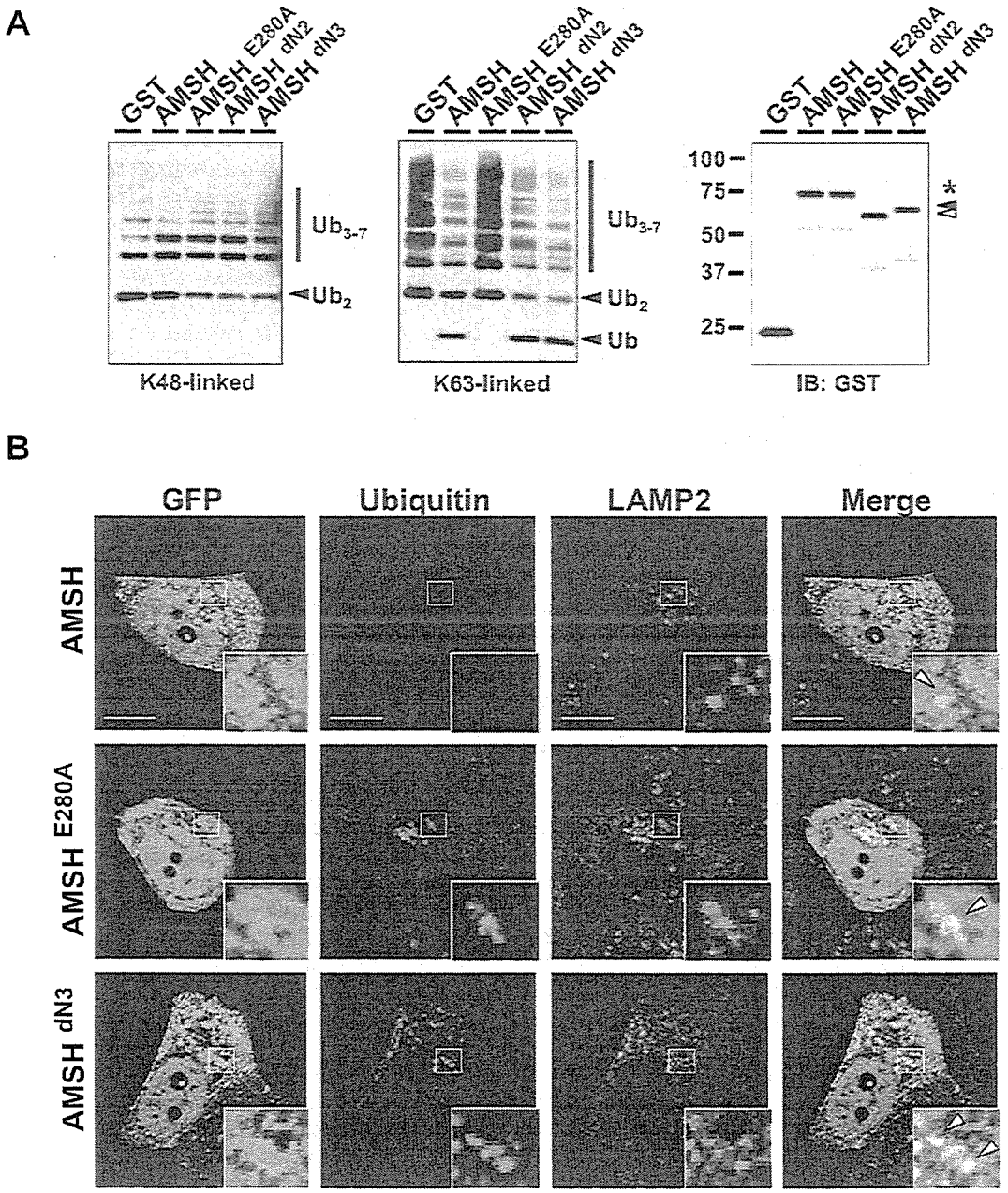


**Fig. 3.** *In vivo* DUB activity of AMSH requires CHMP3-binding capability. (A) CHMP3-binding incapable AMSH mutants retained their deubiquitination activity for K63-linked ubiquitin chains. K48-linked (top) and K63-linked (middle) polyubiquitin chains (Ub2-7) were treated for 18 hours at 37°C with the indicated recombinant protein purified from *E. coli*. Samples were immunoblotted with an anti-ubiquitin mAb, P4D1. Polyubiquitin ($Ub_{3-7}$), diubiquitin ($Ub_2$), and monoubiquitin (Ub) are indicated. Recombinants were immunoblotted with the anti-GST antibody (right panel). (Asterisk, GST-AMSH and GST-AMSH$^{E280A}$; black arrowhead, GST-AMSH$^{dN3}$; white arrowhead, AMSH$^{dN2}$) (B) Accumulation of ubiquitinated protein on late endosomes following the introduction of the mutant AMSH. HeLa cells were transfected with the pEGFP-AMSH, pEGFP-AMSH$^{E280A}$, or pEGFP-AMSH$^{dN3}$. After 48 hours, cells were double-labeled with the indicated primary antibodies FK2 (red) and LAMP2 (blue) are shown. Insets show magnification of boxed areas. Arrows indicate colocalization of LAMP2 with GFP-AMSH (Top), GFP-AMSH$^{E280A}$ and ubiquitinated proteins (Middle), GFP-AMSH$^{dN3}$ and ubiquitinated proteins (Bottom). Bars indicate 10 μm.

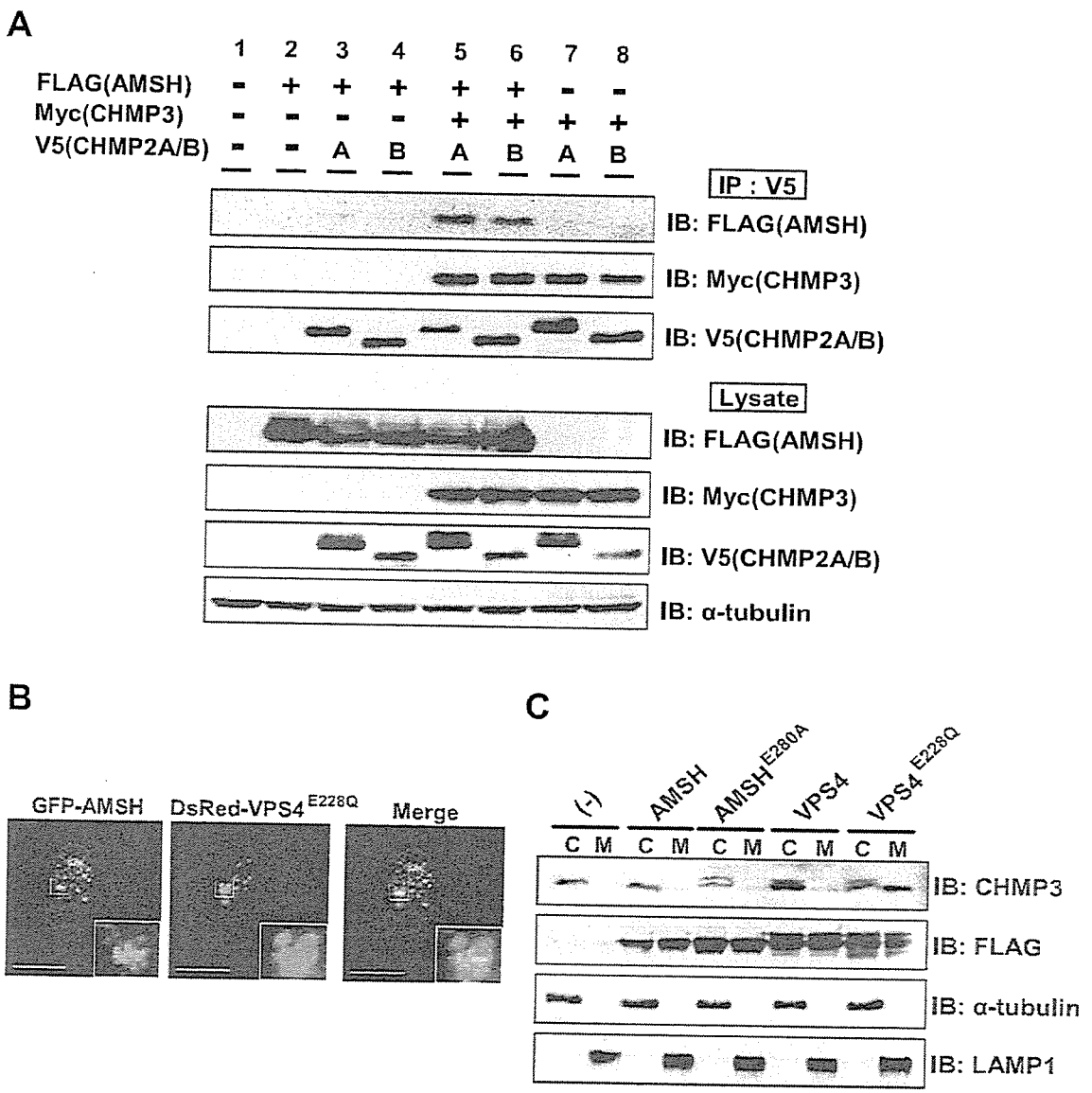


**Fig. 4.** AMSH is included in the ESCRT-III complex *in vivo* and its DUB activity is not essential for the ESCRT-III dissociation. (A) Efficient association of AMSH with CHMP2 requires CHMP3. 293T cells were transfected with p3xFLAG-AMSH, pMyc-CHMP3, and pcDNA3.1-V5-CHMP2, or combinations of them. At 48 hours post-transfection, cell lysates were prepared and used for immunoprecipitation (IP) and immunoblotting (IB) with the indicated antibodies. (B) Co-localization of GFP-AMSH with dominant negative Vps4 in HeLa cells introduced with DsRed-Vps4$^{E228Q}$. HeLa cells were transfected with pEGFP-AMSH and DsRed-Vps4$^{E228Q}$. Bars indicate 10 μm. (C) The catalytic activity of AMSH is not essential for the ESCRT-III dissociation. 293T cells were transfected with p3xFLAG-AMSH, p3xFLAG-AMSH$^{E280A}$, p3xFLAG-VPS4, p3xFLAG-VPS4$^{E228Q}$ or a mock plasmid. Forty-eight hours later, the membrane and cytosolic fractions were prepared and used for immunoblotting with the indicated antibodies. C and M indicate the cytosolic and membrane fraction, respectively. The anti-V5 antibody recognizes the V5 tag on the indicated proteins.

endosome, we next investigated whether gene silencing of AMSH by shRNA affected the intracellular status of ubiquitinated cargo. First, we showed that two sets of our shRNA indeed depleted the cells of AMSH (Fig. 5A). Next, we investigated the ubiquitinated cargo deposition on/within endosomes by using confocal imaging. In the control shRNA-transduced cells, although scattered expression of the endogenous AMSH merged partially with LAMP2, we detected little if any deposits of ubiquitinated cargo that were localized to late endosomes (Fig. 5B, upper panels). On the other hand, in AMSH-depleted cells, a significant deposit of ubiquitinated cargo co-localized with LAMP2-positive endosomes (Fig. 5B middle and lower panels). We observed similar phenotype by using two independent

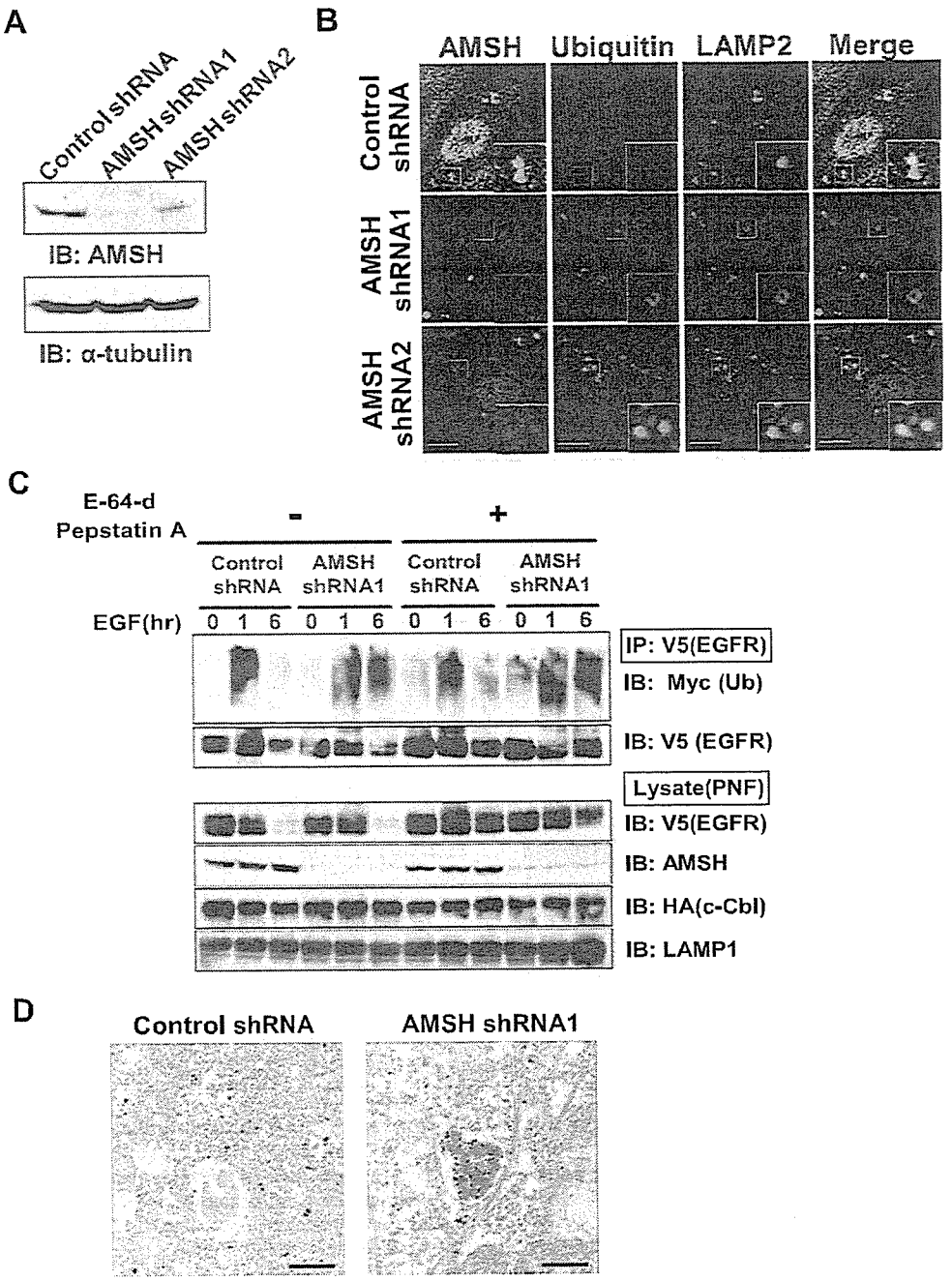


**Fig. 5.** AMSH is essential for the deubiquitination of cargo before its degradation. (A) Depletion of AMSH in HeLa cells. Cells were infected with retrovirus bearing the AMSH-specific shRNA. Immunoblotting was performed with anti-AMSH (top) or anti-α-tubulin antibodies (bottom). (B) HeLa cells depleted of AMSH manifested deposits of ubiquitinated cargo on late endosomes. Cells were fixed and triple-labeled with the indicated antibodies: AMSH (green), FK2 (red), LAMP2 (blue). Insets show magnification of boxed areas. Bars indicate 10 μm. (C) AMSH is essential for the deubiquitination of EGFR. 293T cells were infected with retrovirus bearing the shRNA for AMSH, and transfected with pcDNA3.1-V5-EGFR, pcDNA3.1-Myc-Ubiquitin, and HA-c-Cbl, an E3 ligase that ubiquitinates EGFR. At 48 hours post-stimulation, membrane fractions were prepared and used for immunoprecipitation (IP) and immunoblotting (IB) with the indicated antibodies. (D) Endosomes in AMSH-depleted HeLa cells contain ubiquitinated cargo. HeLa cells depleted of AMSH by shRNA were observed by immuno-EM with the FK2 mAb. Bars indicate 500 nm.

shRNA, suggesting that the observed ubiquitin deposition is not an off-target effect, and hereafter we used shRNA1 for further experiments. Notably, under the AMSH-depletion condition, the number of LAMP2-positive aberrant endosomes containing ubiquitinated cargo was noticeably greater than in the control (Fig. 5B). Collectively, these results suggest that AMSH depletion induces the formation of deposits of ubiquitinated cargo within the LAMP2-positive aberrant endosomes.

To elucidate the role of AMSH in cargo deubiquitination, we next examined whether AMSH affects EGF receptor (EGFR) ubiquitination within the membrane fraction, because EGFR is one of the most intensively studied cargo proteins. To detect EGFR, which is sorted into late endosomes, two lysosome inhibitors, E-64-d and Pepstatin A, were simultaneously added to 293T cells that had been infected with retrovirus bearing the AMSH-specific or control shRNA. To clarify the role of AMSH in ubiquitinated EGFR, we co-expressed c-Cbl in the 293T cells. The level of the exogenously introduced EGFR in the membrane fraction was monitored before and after stimulation with EGF. In the absence of the lysosome inhibitors, robust ubiquitination of EGFR was clearly detected irrespective of AMSH expression 1 hour after the stimulation (Fig. 5C, top panel). At the 6-hour time point, however, ubiquitinated EGFR was observed in the AMSH-depleted lane, but not in the control lane. Under this condition, EGFR degradation was about the same regardless of the presence of AMSH (Fig. 5C, lower panel). In sharp contrast, in the presence of the lysosome inhibitors, EGFR degradation was inhibited, irrespective of AMSH, even at the 6-hour time point. Notably, in the AMSH-depleted samples, EGFR ubiquitination at the 6-hour time point was as strong as at the 1-hour time point. These results suggest that AMSH is essential for the cargo deubiquitination at some time well after EGF stimulation, but may not be required for EGFR degradation.

To investigate the ubiquitinated cargo sorting, we transduced HeLa cells with the AMSH-shRNA. Using samples prepared simultaneously, we performed immuno-electromicroscopy (EM) analysis using the FK2 antibody. In the AMSH-depleted HeLa cells, MVB containing ubiquitinated cargo were observed, while little or no FK2-positve cargo was found in the control cells (Fig. 5D). We concluded that, in the absence of AMSH, ubiquitinated cargo is internalized by the MVB, by invagination, and sorted into the intraluminal vesicles within the MVB without being deubiquitinated. Collectively, these results suggest that ubiquitinated cargo, including EGFR, is deubiquitinated by AMSH before the cargo's lysosome-dependent degradation.

## *Discussion*

In this study, we provide evidence that AMSH binds ESCRT-III. As was expected from its high homology to yeast Vps24p, CHMP3 is now known to be a mammalian ESCRT-III subunit (Howard *et al.*, 2001). Our present conclusion that AMSH binds CHMP3 is consistent with reports by others (Agromayor and Martin-Serrano, 2006; McCullough *et al.*, 2006), and similar binding has been identified between *Drosophila* orthologues of these molecules (Giot *et al.*, 2003). Although genetic evidence has already proven that ESCRT-III functions downstream of ESCRT-II in sorting and concentrating the ubiquitinated cargo of the MVB/late endosome (Bowers *et al.*, 2004), the involvement of a DUB in mammalian MVB sorting had not been clarified previously. Therefore, our present data, along with recent report from others, provide important insights that support the hypothesis that mammalian protein sorting relies on DUB activity.

The association of AMSH with CHMP3 requires AMSH's amino-terminal region, spanning residues 1–82 ($AMSH^{1-82}$, Fig. 1D). Because earlier reports indicated that $AMSH^{1-103}$, which includes the MIT-like domain ($AMSH^{34-97}$), is required for CHMP3 binding (McCullough *et al.*, 2006; Tsang *et al.*, 2006), our present study has further refined the responsible region. However, we found that the localization of AMSH to endosomes does not depend on the CHMP3 association (Fig. 2B). Nonetheless, clathrin heavy chain (CHC) is also known to bind AMSH (McCullough *et al.*, 2006; Nakamura *et al.*, 2006), and therefore may play some role in its localization to late endosomes, as well as its reported localization to early endosomes. Furthermore, because we repeatedly observed an increased recruitment of AMSH to endosomes in cells expressing CHMP3 (data not shown), we speculate that, although CHMP3 is not required, it may have at least an auxiliary function to support the recruitment of AMSH to endosomes (Fig. 2B). Our findings are consistent with a recent report demonstrating the efficient recruitment of AMSH to CHMP1/3-positive endosomes by the forced expression of an ESCRT-III subunit, CHMP1/3 (Agromayor and Martin-Serrano, 2006; Tsang *et al.*, 2006). It is possible that a combination of multiple associated proteins, including CHC and the CHMPs, may determine the recruitment of AMSH onto endosomes. In the present study, we also found that AMSH is involved in the CHMP3-CHMP2 complex, which may act as a subunit of the ESCRT-III complex (Fig. 4A). Since AMSH binds CHMP2 in the absence of exogenous CHMP3, AMSH may bind CHMP2 with less affinity, although we cannot fully rule out the possibility that endogenous CHMP3 mediates indirect binding between AMSH and CHMP2. In line with the former possibility, a recent report demonstrated direct binding between CHMP2A and AMSH (Agromayor and Martin-Serrano, 2006). In any case, our present data indicate that CHMP3 enhances the association between CHMP2 and AMSH.

We previously documented that AMSH binds STAM. Therefore, it is interesting to speculate whether the ternary complex, STAM-AMSH-CHMP3, exists *in vivo*. Indeed,

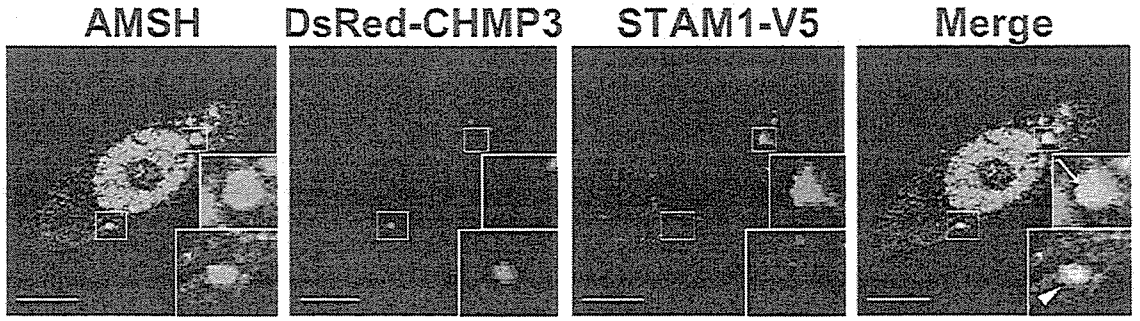


**Supplementary Fig. S2.** Co-localizations of AMSH-STAM and AMSH-CHMP3 exist in a mutually independent manner. HeLa cells were transfected with pDsRed-Monomer-CHMP3 and STAM1-V5. After 48 hours, cells were double-labeled with the antibodies indicated on the figure. AMSH (green), DsRed-CHMP3 (red), and STAM1-V5 (blue). Arrowheads indicate localization of AMSH in DsRed-CHMP3-positive aberrant endosomes. Arrows indicate localization of AMSH in STAM1-V5-positive aberrant endosomes. Bars indicate 10 μm.

by co-immunoprecipitation experiments, we observed this three-molecule complex (data not shown). However, under confocal imaging, we repeatedly detected more frequent colocalization of AMSH-STAM to early endosomes (data not shown), whereas the AMSH-CHMP3 complex showed localization to MVB/late endosomes (Fig. 2A). In addition, we found that colocalizations of AMSH-STAM and AMSH-CHMP3 exist in a mutually independent manner (Supplementary Fig. S2). Although associations of AMSH with CHMP1, 2, and 3 have been reported, the localization of these complexes was unknown. Therefore, our present data is the first to identify the late endosomal localization of AMSH, supporting our hypothesis that AMSH functions within the ESCRT-III complex. Further experiments should reveal whether a multi-ESCRT complex including the ESCRT-0 (STAM/Hrs), -I, -II, and -III exists. In any case, a requirement for a binding partner for AMSH to carry out its *in vivo* functions may explain the diverse roles of AMSH, as well as its localization to early endosomes and the nucleus.

We found that AMSH$^{dN3}$ expression in HeLa cells resulted in a remarkable deposition of ubiquitinated proteins that colocalized with aberrant LAMP1/EEA1-double positive endosomes, despite AMSH$^{dN3}$'s retaining its *in vitro* DUB activity (Fig. 2 and Fig. 3). In AMSH$^{dN3}$-introduced cells, approximately 95% of EEA1-positive vesicles and 80% of the LAMP2-positive vesicles contained ubiquitinated cargo. We speculate that a certain percentage of the ubiquitinated cargo accumulated in the EEA1/LAMP2-double positive endosomes. The less frequent accumulation within the late endosome may be an outcome of a possible degradation of ubiquitinated cargo within the vesicle. Ubiquitin deposition in the presence of AMSH$^{dN3}$ was similar to that observed when AMSH$^{E280A}$ was expressed, or the endogenous AMSH was depleted (Fig. 3 and Fig. 5). Therefore, although we cannot fully exclude the possibility that ESCRT-III proteins other than CHMP3 may be involved in the ubiquitin deposition resulting from AMSH$^{dN3}$ expression, we speculate that substrate recognition by AMSH requires CHMP3 binding, at least on late endosomes. In any case, the formation of a complex between CHMP3 and AMSH seems to be essential for the deubiquitination of endosome cargo proteins. In support of this assumption, other JAMM domain-containing isopeptidases, such as Rpn11 and CSN5, also function within complexes (Cope *et al.*, 2002; Verma *et al.*, 2002; Yao and Cohen, 2002). Indeed, there may be a difference among DUBs in terms of their mode of action: one group may function by direct recognition of their substrates, while the other group, including the JAMM domain-containing isopeptidases, may function as a constituent of a complex (Amerik and Hochstrasser, 2004). The unique structures of the catalytic regions of the DUBs, as well as the presence of specific sets of interaction domains in the different DUBs may explain such differences (Ambroggio *et al.*, 2004). Interestingly, unlike the ESCRT-0, -I, and -II components, ESCRT-III constituents seem to lack previously identified ubiquitin-binding motifs. Including AMSH in the complex could result in efficient cargo deubiquitination, since ESCRT-III has access to the ubiquitin moieties on the cargo proteins. Interestingly, a recent report demonstrated that the *in vitro* DUB activity of AMSH is augmented when AMSH is bound to STAM (McCullough *et al.*, 2006). However, binding CHMP3 did not strengthen AMSH's DUB activity (McCullough *et al.*, 2006). In addition to cargo proteins, it is also possible that ESCRT proteins themselves could be included in the vesicle as ubiquitinated proteins, because ubiquitination of Hrs is reported (Hoeller *et al.*, 2006). It will be intriguing to determine the content of vesicle to clarify the property of the ubiquitinated proteins.

McCullough *et al.* (2004) previously documented that AMSH deubiquitinates EGFR *in vitro* but is not essential for its sorting/degradation *in vivo*. In this study, we found that AMSH is responsible for the EGFR deubiquitination *in vivo* at time points well after (6 hr) EGF stimulation (Fig. 5C). In our EM analysis, an accumulation of ubiquitinated cargo was identified within MVB in AMSH-depleted cells (Fig. 5D). This is consistent with previous findings in yeast

that deubiquitination by Doa4 is not essential for cargo sorting into vacuoles (Amerik *et al.*, 2000). Instead, in Doa4 mutants, intracellular free ubiquitins are depleted by the insufficiency of Doa4-function, which cleaves ubiquitin chains to produce free ubiquitins (Swaminathan *et al.*, 1999). In our hands, however, we detected little if any decrease in the intracellular free ubiquitin regardless of AMSH expression (data not shown). One possible explanation is that there may be a redundant DUB activity in mammals. Recently, a DUB called UBPY was suspected as a possible Doa4 orthologue in mammals, but the same report showed that the amount of free ubiquitin in UBPY-depleted cells was unaltered (Mizuno *et al.*, 2005). In addition, there is no evidence so far supporting UBPY's involvement in ESCRT-III. Therefore, we assume that an as yet unidentified ESCRT-III-related DUB(s) is essential for the ubiquitin turnover. One such candidate is AMSH-LP, an AMSH-related DUB (Kikuchi *et al.*, 2003). Although AMSH-LP is located on early endosomes and catalytically inactive AMSH-LP induces ubiquitinated cargo accumulation (Nakamura *et al.*, 2006), AMSH-LP seems not to be included in the ESCRT-III complex (Agromayor and Martin-Serrano, 2006), our unpublished data). Although further experiments are needed to identify DUBs that strictly meet the criteria for being a yeast DUB orthologue, we tentatively speculate that AMSH functionally corresponds to Doa4.

In conclusion, we demonstrated that not only the DUB activity of AMSH but also its CHMP3-binding capability is required for the *in vivo* function of AMSH. AMSH depletion results in the formation of aberrant endosomes in cells. Further *in vivo* analyses of DUBs should continue to provide new insights into their specific roles in mammals.

*Acknowledgements.* This work was supported in part by a Grant-in-Aid for Scientific Research from the Japan Society for the Promotion of Science (JSPS), a Grant-in-Aid for Scientific Research in Priority Areas and a Grant-in-Aid for a Center of Excellence (COE) program from the Ministry of Education, Science, Sports and Culture of the Japanese Government, and a Grant-in-Aid from the Takeda Medical Research Foundation. M.K. is supported by a Grant-in-Aid for JSPS Fellows.

***References***

Agromayor, M. and Martin-Serrano, J. 2006. Interaction of AMSH with ESCRT-III and deubiquitination of endosomal cargo. *J. Biol. Chem.*, **281**: 23083–23091.

Ambroggio, X.I., Rees, D.C., and Deshaies, R.J. 2004. JAMM: a metallo-protease-like zinc site in the proteasome and signalosome. *PLoS Biol.*, **2**: E2.

Amerik, A.Y. and Hochstrasser, M. 2004. Mechanism and function of deubiquitinating enzymes. *Biochim. Biophys. Acta*, **1695**: 189–207.

Amerik, A.Y., Nowak, J., Swaminathan, S., and Hochstrasser, M. 2000. The Doa4 deubiquitinating enzyme is functionally linked to the vacuolar protein-sorting and endocytic pathways. *Mol. Biol. Cell*, **11**: 3365–3380.

Asao, H., Sasaki, Y., Arita, T., Tanaka, N., Endo, K., Kasai, H., Takeshita, T., Endo, Y., Fujita, T., and Sugamura, K. 1997. Hrs is associated with STAM, a signal-transducing adaptor molecule. Its suppressive effect on cytokine-induced cell growth. *J. Biol. Chem.*, **272**: 32785–32791.

Babst, M. 2005. A protein's final ESCRT. *Traffic*, **6**: 2–9.

Babst, M., Katzmann, D.J., Estepa-Sabal, E.J., Meerloo, T., and Emr, S.D. 2002. Escrt-III: an endosome-associated heterooligomeric protein complex required for mvb sorting. *Dev. Cell*, **3**: 271–282.

Babst, M., Sato, T.K., Banta, L.M., and Emr, S.D. 1997. Endosomal transport function in yeast requires a novel AAA-type ATPase, Vps4p. *EMBO J.*, **16**: 1820–1831.

Babst, M., Wendland, B., Estepa, E.J., and Emr, S.D. 1998. The Vps4p AAA ATPase regulates membrane association of a Vps protein complex required for normal endosome function. *EMBO J.*, **17**: 2982–2993.

Bonifacino, J.S. and Traub, L.M. 2003. Signals for sorting of transmembrane proteins to endosomes and lysosomes. *Annu. Rev. Biochem.*, **72**: 395–447.

Bowers, K., Lottridge, J., Helliwell, S.B., Goldthwaite, L.M., Luzio, J.P., and Stevens, T.H. 2004. Protein-protein interactions of ESCRT complexes in the yeast Saccharomyces cerevisiae. *Traffic*, **5**: 194–210.

Cope, G.A., Suh, G.S., Aravind, L., Schwarz, S.E., Zipursky, S.L., Koonin, E.V., and Deshaies, R.J. 2002. Role of predicted metalloprotease motif of Jab1/Csn5 in cleavage of Nedd8 from Cul1. *Science*, **298**: 608–611.

Fujimuro, M., Sawada, H., and Yokosawa, H. 1994. Production and characterization of monoclonal antibodies specific to multi-ubiquitin chains of polyubiquitinated proteins. *FEBS Lett.*, **349**: 173–180.

Giot, L., Bader, J.S., Brouwer, C. *et al.* 2003. A protein interaction map of Drosophila melanogaster. *Science*, **302**: 1727–1736.

Glickman, M.H. and Ciechanover, A. 2002. The ubiquitin-proteasome proteolytic pathway: destruction for the sake of construction. *Physiol. Rev.*, **82**: 373–428.

Gruenberg, J. and Stenmark, H. 2004. The biogenesis of multivesicular endosomes. *Nat. Rev. Mol. Cell Biol.*, **5**: 317–323.

Hicke, L. 2001. A new ticket for entry into budding vesicles-ubiquitin. *Cell*, **106**: 527–530.

Hoeller, D., Crosetto, N., Blagoev, B., Raiborg, C., Tikkanen, R., Wagner, S., Kowanetz, K., Breitling, R., Mann, M., Stenmark, H., and Dikic, I. 2006. Regulation of ubiquitin-binding proteins by monoubiquitination. *Nat. Cell Biol.*, **8**: 163–169.

Howard, T.L., Stauffer, D.R., Degnin, C.R., and Hollenberg, S.M. 2001. CHMP1 functions as a member of a newly defined family of vesicle trafficking proteins. *J. Cell Sci.*, **114**: 2395–2404.

Itoh, F., Asao, H., Sugamura, K., Heldin, C.H., ten Dijke, P., and Itoh, S. 2001. Promoting bone morphogenetic protein signaling through negative regulation of inhibitory Smads. *EMBO J.*, **20**: 4132–4142.

Kanazawa, C., Morita, E., Yamada, M., Ishii, N., Miura, S., Asao, H., Yoshimori, T., and Sugamura, K. 2003. Effects of deficiencies of STAMs and Hrs, mammalian class E Vps proteins, on receptor down-regulation. *Biochem. Biophys. Res. Commun.*, **309**: 848–856.

Katzmann, D.J., Babst, M., and Emr, S.D. 2001. Ubiquitin-dependent sorting into the multivesicular body pathway requires the function of a conserved endosomal protein sorting complex, ESCRT-I. *Cell*, **106**: 145–155.

Katzmann, D.J., Odorizzi, G., and Emr, S.D. 2002. Receptor downregulation and multivesicular-body sorting. *Nat. Rev. Mol. Cell Biol.*, **3**: 893–905.

Kikuchi, K., Ishii, N., Asao, H., and Sugamura, K. 2003. Identification of AMSH-LP containing a Jab1/MPN domain metalloenzyme motif. *Biochem. Biophys. Res. Commun.*, **306**: 637–643.

Kobayashi, H., Tanaka, N., Asao, H., Miura, S., Kyuuma, M., Semura, K., Ishii, N., and Sugamura, K. 2005. Hrs, a mammalian master molecule in vesicular transport and protein sorting, suppresses the degradation of ESCRT proteins signal transducing adaptor molecule 1 and 2. *J. Biol. Chem.*, **280**: 10468–10477.

Kobayashi, T., Stang, E., Fang, K.S., de Moerloose, P., Parton, R.G., and Gruenberg, J. 1998. A lipid associated with the antiphospholipid

syndrome regulates endosome structure and function. *Nature*, **392**: 193–197.

Luhtala, N. and Odorizzi, G. 2004. Bro1 coordinates deubiquitination in the multivesicular body pathway by recruiting Doa4 to endosomes. *J. Cell Biol.*, **166**: 717–729.

McCullough, J., Clague, M.J., and Urbe, S. 2004. AMSH is an endosome-associated ubiquitin isopeptidase. *J. Cell Biol.*, **166**: 487–492.

McCullough, J., Row, P.E., Lorenzo, O., Doherty, M., Beynon, R., Clague, M.J., and Urbe, S. 2006. Activation of the endosome-associated ubiquitin isopeptidase AMSH by STAM, a component of the multivesicular body-sorting machinery. *Curr. Biol.*, **16**: 160–165.

Mizuno, E., Iura, T., Mukai, A., Yoshimori, T., Kitamura, N., and Komada, M. 2005. Regulation of epidermal growth factor receptor down-regulation by UBPY-mediated deubiquitination at endosomes. *Mol. Biol. Cell*, **16**: 5163–5174.

Mizuno, E., Kawahata, K., Kato, M., Kitamura, N., and Komada, M. 2003. STAM proteins bind ubiquitinated proteins on the early endosome via the VHS domain and ubiquitin-interacting motif. *Mol. Biol. Cell*, **14**: 3675–3689.

Morita, E. and Sundquist, W.I. 2004. Retrovirus budding. *Annu. Rev. Cell Dev. Biol.*, **20**: 395–425.

Nakamura, M., Tanaka, N., Kitamura, N., and Komada, M. 2006. Clathrin anchors deubiquitinating enzymes, AMSH and AMSH-like protein, on early endosomes. *Genes Cells*, **11**: 593–606.

Raiborg, C., Rusten, T.E., and Stenmark, H. 2003. Protein sorting into multivesicular endosomes. *Curr. Opin. Cell Biol.*, **15**: 446–455.

Swaminathan, S., Amerik, A.Y., and Hochstrasser, M. 1999. The Doa4 deubiquitinating enzyme is required for ubiquitin homeostasis in yeast. *Mol. Biol. Cell*, **10**: 2583–2594.

Tanaka, N., Kaneko, K., Asao, H., Kasai, H., Endo, Y., Fujita, T., Takeshita, T., and Sugamura, K. 1999. Possible involvement of a novel STAM-associated molecule "AMSH" in intracellular signal transduction mediated by cytokines. *J. Biol. Chem.*, **274**: 19129–19135.

Tsang, H.T., Connell, J.W., Brown, S.E., Thompson, A., Reid, E., and Sanderson, C.M. 2006. A systematic analysis of human CHMP protein interactions: additional MIT domain-containing proteins bind to multiple components of the human ESCRT III complex. *Genomics*, **88**: 333–346.

Verma, R., Aravind, L., Oania, R., McDonald, W.H., Yates, J.R., 3rd, Koonin, E.V., and Deshaies, R.J. 2002. Role of Rpn11 metalloprotease in deubiquitination and degradation by the 26S proteasome. *Science*, **298**: 611–615.

Weissman, A.M. 2001. Themes and variations on ubiquitylation. *Nat. Rev. Mol. Cell Biol.*, **2**: 169–178.

Yao, T. and Cohen, R.E. 2002. A cryptic protease couples deubiquitination and degradation by the proteasome. *Nature*, **419**: 403–407.

Yoshimori, T., Yamagata, F., Yamamoto, A., Mizushima, N., Kabeya, Y., Nara, A., Miwako, I., Ohashi, M., Ohsumi, M., and Ohsumi, Y. 2000. The mouse SKD1, a homologue of yeast Vps4p, is required for normal endosomal trafficking and morphology in mammalian cells. *Mol. Biol. Cell*, **11**: 747–763.

*(Received for publication, August 23, 2006*
*and accepted, November 20, 2006)*

International Immunology, Vol. 18, No. 2, pp. 269–277
doi:10.1093/intimm/dxh366

© The Japanese Society for Immunology. 2005. All rights reserved.
For permissions, please e-mail: journals.permissions@oxfordjournals.org

# Regulatory T cell-like activity of Foxp3$^+$ adult T cell leukemia cells

**Shuming Chen[1], Naoto Ishii[1], Shouji Ine[1], Syuichi Ikeda[2], Taku Fujimura[3], Lishomwa C. Ndhlovu[1], Pejman Soroosh[1], Kohtaro Tada[1], Hideo Harigae[4], Junichi Kameoka[4], Noriyuki Kasai[5], Takeshi Sasaki[4]** and **Kazuo Sugamura[1]**

[1]Department of Microbiology and Immunology, Tohoku University Graduate School of Medicine, Sendai 980-8575, Japan
[2]Sasebo City General Hospital, Sasebo 857-8511, Japan
[3]Department of Dermatology, [4]Department of Rheumatology and Hematology and [5]Institute for Animal Experimentation, Tohoku University Graduate School of Medicine, Sendai 980-8575, Japan

*Keywords*: ATL, Foxp3, HTLV-I, regulatory T cell

## Abstract

**Adult T cell leukemia (ATL) is an aggressive neoplastic disease, in which a quarter of the patients develop opportunistic infections due to cellular immunodeficiency. However, the underlying mechanism responsible for the immunosuppression has remained unclear. Recent studies have demonstrated that the leukemia cells from a subset of patients with ATL express Foxp3, a specific marker for CD25$^+$CD4$^+$ regulatory T (Treg) cells, which regulate the immune response by suppressing CD4$^+$ T cell functions. However, whether there is a functional resemblance between ATL cells that have Foxp3 expression and Treg cells is still unknown. In this report, we confirmed the high expression of Foxp3 in leukemia cells from 5 of 12 ATL patients and demonstrated that ATL cells from 3 patients suppressed the proliferation of CD4$^+$ T cells. Similarly, one of six HTLV-I-infected cell lines showed both high Foxp3 expression and suppressive activity. Like Treg cells, the suppression induced by the ATL cells from two patients and the HTLV-infected cell line appeared to be mediated by a cell–cell contact-dependent mechanism. Nevertheless, among the ATL cells that strongly expressed Foxp3, those from two of the five patients showed no apparent suppressive activity. Furthermore, retroviral transfection of Foxp3 did not confer any suppressive function on low Foxp3-expressing HTLV-I-infected cell lines. These results indicate that Foxp3 may be essential but is not sufficient for the Treg-cell-like suppressive activity of ATL cells and HTLV-I-infected cell lines.**

## Introduction

Adult T cell leukemia (ATL) is a progressive peripheral T lymphocytic malignancy strongly associated with human T cell leukemia virus type 1 (HTLV-I) infection (1, 2). A quarter of ATL patients develop overwhelming opportunistic infections (pneumocystis carinii, cytomegalovirus and fungal infections) as a consequence of defective cellular immunity (2–4). Since patients with ATL do not exhibit bone marrow depression, a well recognized cause of immunodeficiency in other types of leukemia (2, 5), the mechanism(s) may be associated with peripheral immunodeficiency. Nevertheless, the reason for immunosuppression in ATL remains unclear.

Most ATL cells express the helper T cell-associated antigen CD4 and the T cell activation marker CD25 (2, 6). Several previous studies have demonstrated that established HTLV-I-infected T cell lines have characteristics similar to activated CD4 T cells, in terms of their expression of IL-2 receptor subunits and T cell activation markers, such as CD25 and OX40 (2, 6). Thus, leukemia cells in patients with ATL have been thought to be derived from activated CD4 T cells. CD4 and CD25, however, are also characteristic of CD25$^+$CD4$^+$ regulatory T (Treg) cells. Treg cells have been identified recently in both mice and humans as naturally arising professional suppressor T cells that are capable of inhibiting the *in vitro* proliferation of CD25$^-$CD4$^+$ T cells stimulated via TCRs (7, 8). In addition, a number of *in vivo* studies in mice have demonstrated that Treg cells can control autoimmune disorders, allograft tolerance and tumor immunity by suppressing T cell-mediated responses (7–9). Despite expressing TCRs and surface IL-2 receptors, Treg cells remain anergic to stimulation via their TCRs. Similarly, most ATL cells are unable

*Correspondence to*: N. Ishii; E-mail: ishiin@mail.tains.tohoku.ac.jp

*Transmitting editor*: T. Saito

*Received* 8 September 2005, *accepted* 4 November 2005

Advance Access publication 16 December 2005

to mount a full proliferation response to TCR ligation, even though they too express these receptors. In addition to these similarities between ATL and Treg cells, recent papers have demonstrated that Foxp3, a Treg-cell-specific transcription factor, is expressed in the leukemia cells from a subset of patients with ATL (10–13). Foxp3 expression is indispensable for the development and function of Treg cells (7). From these findings, we hypothesized that the Foxp3-expressing ATL cells may have suppressive activity, and that some of them might have been derived from Treg cells instead of from activated T cells. To address this, we have examined the phenotypic characteristics and immunosuppressive activity of leukemia cells from 12 patients with ATL, and compared them to those of freshly isolated Treg cells and HTLV-I-infected T cell lines. Furthermore, we have investigated the functional association between Foxp3 expression and suppressive function in HTLV-I-infected cell lines retrovirally transfected with the Foxp3 gene.

## Methods

### *Cases*

Twelve ATL patients of various ages from Sasebo City General Hospital (Sasebo, Japan) and Tohoku University Hospital (Sendai, Japan) were recruited for this study (Table 1). The diagnosis of ATL was confirmed by the microscopic examination of peripheral blood cells. Furthermore, all of the patients had confirmed positive tests for serum antibodies against ATL antigen. ATL cells ($CD25^+CD4^+$ cells) comprised >80% of the PBMCs in most of the patients (Table 1). Among the acute ATL patients, two were demonstrably immunocompromised, even though they, like most of the patients, were receiving appropriate anti-microbial and anti-fungal treatment (Table 1).

### *Cell lines*

The ILT-Mat, TCL-Mor, TCL-Kan and MT-2 cell lines are *in vitro*-established HTLV-I-infected $CD4^+$ T cell lines described previously (14, 15). TL-Om1 and EDγ-16 were derived from leukemia cells isolated from patients with ATL (14, 16, 17). JPX9, which is an HTLV-I *tax* transfectant cell line derived from Jurkat, a human acute lymphocytic leukemia T cell line, was previously described (18). In brief, JPX9 cells were established by stably introducing a metallothionein promoter-directed p40*tax* expression vector, pMAXRHneo-I, into Jurkat cells. Thus, the p40*tax* product could be induced in response to $CdC1_2$ in these cells. Tax expression in JPX9 cells was confirmed by reverse transcription (RT)–PCR as described previously (19). These cells were maintained in RPMI 1640 medium supplemented with 10% FCS, 100 U $ml^{-1}$ penicillin and 100 μg $ml^{-1}$ streptomycin. The ILT-Mat culture medium included 500 nM recombinant human IL-2 (Ajinomoto, Kanagawa).

### *Retroviral transduction with the Foxp3 gene*

To establish lines from cells transfected with the Foxp3 gene, human full-length Foxp3 cDNA was cloned from primary Treg cells and inserted into a GFP-expressing retrovirus vector pMXs-IG, yielding pMXs-IG-Foxp3. Packaging cells were transfected with the pMXs-IG-Foxp3 plasmid by $Ca_3(PO_4)_2$ precipitation. The retrovirus-containing supernatant was collected after a 48-h culture at 37°C. EDγ-16 and ILT-Mat were suspended in the retrovirus-containing supernatant, spun for 60 min at 1200 × *g* and cultured in the complete medium. After 2 weeks of culture, the GFP-positive cells were isolated by FACSAria (BD, Bioscience). The cloning primers for the full-length Foxp3 cDNA were forward primer 5′-CCGCTCGAGCAAGGACCCGATGCCCAACC and reverse primer 5′-CCGCTCGAGCTCTGCCTCCCACCAGTTTG.

### *In vitro T cell responses*

$CD4^+$ T cells were isolated from PBMCs by using a $CD4^+$ T cell Isolation Kit (Miltenyi Biotec, Gladbach, Germany). $CD25^+CD4^+$ Treg and conventional $CD25^-CD4^+$ T cells were labeled with anti-CD25-biotin (IMMUNOTECH, Marseille Cedex, France) and further separated by an AutoMACS (Miltenyi Biotec). Purified $CD25^-CD4^+$ T cells ($5 \times 10^4$) were stimulated with 10 μg $ml^{-1}$ soluble anti-CD3 mAb for 5 days in the presence of PBMC-derived dendritic cells (DCs; $5 \times 10^3$). To prepare DCs, monocytes were isolated from PBMCs by plastic adherence and cultured in X-VIVO-15 (BioWhittaker, Walkersille, MD) supplemented with 30 ng $ml^{-1}$ IL-4 and granulocyte macrophage colony-stimulating factor (PeproTech, London, UK) for 7 days. To prepare ATL cells, whole PBMCs from all the patients except for patient 11 were used as ATL cells because leukemia cells comprised 80–96% of

**Table 1.** ATL patient data

| Case ID | Sex | Age | Clinical type | Clinical course | WBC ($10^3$ $\mu l^{-1}$) | Proportion of ATL cells in PBMCs (%) | Infectious complication |
|---|---|---|---|---|---|---|---|
| 1 | M | 44 | Acute | Onset | 10.9 | 92 | Cutaneous infection |
| 2 | M | 75 | Acute | Relapse | 10.4 | 88 | Oral candida |
| 3 | M | 62 | Acute | Onset | 145.5 | 90 | No |
| 4 | M | 70 | Acute | Relapse | 8.4 | 97 | No |
| 5 | M | 41 | Acute | Onset | 102.8 | 90 | No |
| 6 | M | 58 | Chronic | Onset | 177 | 96 | No |
| 7 | F | 68 | Acute | Onset | 58 | 83 | No |
| 8 | M | 69 | Chronic | Onset | 19.5 | 82 | No |
| 9 | M | 69 | Chronic | Remission | 60.3 | 94 | No |
| 10 | F | 55 | Acute | Onset | 39 | 90 | No |
| 11 | M | 68 | Acute | Onset | 9.9 | 47 | No |
| 12 | M | 58 | Acute | Onset | 13.4 | 80 | No |

PBMC in 11 of the 12 patients (see Table 1). In the case of patient 11, in whom leukemic cells accounted for 43% of PBMC, $CD25^+CD4^+$ cells were purified as described above. Purified $CD25^+CD4^+$ T (Treg) or ATL cells were added to the culture at the indicated dose. After 5 days of culture, the $CD25^-CD4^+$ T cells were assayed for $^3$Hthymidine ([$^3$H]TdR) uptake. Alternatively, $CD25^-CD4^+$ T cells were labeled with 5,6-carboxy-fluorescein succinimidyl ester (CFSE) and assayed for CFSE intensity. In some experiments, neutralizing antibody against IL-10 (BD Biosciences), cytotoxic T lymphocyte antigen 4 (CTLA-4) (IMMUNOTECH) or TGFβ (R&D System) (10 μg $ml^{-1}$ each) was added to the culture.

*Trans-well experiments*

$CD25^-CD4^+$ T cells ($2 \times 10^5$) were cultured with DCs ($1 \times 10^4$) in the presence of anti-CD3 mAb (10 μg $ml^{-1}$) in 24-well plates. ATL or Treg cells, and DCs ($1 \times 10^4$) were either added directly to the wells or placed in trans-well chambers. After a 5-day culture, the amount of proliferation of the $CD25^-CD4^+$ T cells was determined by [$^3$H]TdR uptake in 96-well plates. In other proliferation studies, purified $CD25^-CD4^+$ T cells were labeled with CFSE (Molecular Probes, Eugene, OR) by incubation with 2.5 μM CFSE in protein-free PBS for 10 min at 37°C and then with a 10-fold volume of RPMI 1640 medium containing 10% FCS for 1 min. Cells were then washed twice with chilled PBS. The cell division of CFSE-labeled cells was estimated by their decreased fluorescence intensity, using a flow cytometer.

*Establishment of HTLV-I-infected T cell clones derived from $CD25^-CD4^+$ T cells*

Purified $CD25^-CD4^+$ T cells (purity > 99%) from healthy donors were co-cultured with 20 000-rad irradiated MT-2 cells in RPMI 1640 medium supplemented with 10% FCS. Two months later, live cells were collected and cultured at limiting dilution in the presence of IL-2, to establish HTLV-I-infected cell clones. Two clones (4-2 and 4-20) were obtained in two independent infections. These cells were confirmed to be positive for HTLV-I infection by immunostaining with the GIN14 mAb, which recognizes HTLV-I core proteins (6).

*Real-time PCR*

Total RNA was isolated by Trizol Reagent (Invitrogen, Carlsbad, CA), and converted to cDNA by the SuperScript III First-Strand Synthesis System for RT-PCR kit (Invitrogen) using an oligo(dT)15 primer. To detect Foxp3, the TaqMan probe and primer was used. Real-time PCR was performed using an ABI 7700 Sequence Detection System (Applied Biosystem, Foster, CA). The expression of each gene was normalized to the copies of GAPDH mRNA from the same sample.

*Detection of* tax *gene*

Total RNA was isolated from ATL cells and JPX9 cells as described above, and treated with DNase I (Sigma, US) before RT. cDNA was generated from the extracted total RNA as described above. Primers for *tax* (19) are as follows: forward primer 5′-CCCACTTCCCAGGGTTTGGACAGA, reverse primer 5′-CTGTAGAGCTGAGCCGATAACGCG. Primers for GAPDH are as follows: forward primer 5′-CCACATCGCTCAGACAC-CAT, reverse primer 5′-GCCATCACGCCACAGTTTCC.

## Results

*Phenotypic analysis of ATL cells*

To confirm recent observations, we first examined the expression of Foxp3 in leukemia cells isolated from patients with ATL, by real-time PCR. The transcript level of Foxp3 in the ATL cells of 5 of 12 patients (patients 1, 6, 7, 8, and 9) was comparable to the level in freshly isolated Treg cells (Table 2 and Fig. 1A). Similar results were obtained in three recent reports (10–12). In addition, the average Foxp3 expression in ATL cells was significantly higher than that in activated conventional $CD4^+$ T cells, in which low Foxp3 expression was observed (Fig. 1A). Furthermore, no Foxp3 expression in the leukemia cells from a patient with acute T lymphocytic leukemia (T-ALL) could be detected. Thus, from a phenotypic standpoint, we concluded that the ATL cells from more than one-third of the patients we examined resembled Treg cells rather than activated T cells.

*Suppressive activity of ATL cells*

We next examined the suppressive activity of ATL cells on the proliferation and cell division of $CD25^-CD4^+$ (conventional CD4) T cells by determining the levels of DNA synthesis and CFSE intensity, respectively. When cultured at an equal ratio, ATL cells from patients 1, 2 and 9 induced moderate inhibition of the CD3-stimulated $CD25^-CD4^+$ T cell proliferative responses that was less than the inhibition induced by Treg cells (Fig. 1B). In addition, the frequency of cells failing to undergo cell division was higher when ATL cells from patients 1 and 9 were co-cultured (16 and 15%, respectively) than when $CD25^-CD4^+$ T cells alone were added (9%) (Fig. 1C). Furthermore, ATL-cell-induced suppression was markedly enhanced when the ratio of the ATL cells from patients 1 and 9 to $CD25^-CD4^+$ T cells was increased 5-fold (Fig. 1B and C). Interestingly, patient 7's ATL cells, which had the highest Foxp3 expression, did not affect the proliferation or cell division of conventional CD4 T cells, even when a higher ratio of ATL cells was added to the co-culture (Fig. 1B and C).

*Mechanisms responsible for the ATL-cell-mediated suppression*

It has been reported that, following *in vitro* culture, ATL cells secrete the regulatory cytokines IL-10 and TGFβ (19, 20). On

**Table 2.** Phenotypic and functional analysis of ATL cells

| Case ID | Relative Foxp3 expression | Suppressive activity | Expression of Tax |
|---|---|---|---|
| 1 | 12 | + | + |
| 2 | 1.1 | + | + |
| 3 | 2.3 | – | – |
| 4 | 0.32 | – | + |
| 5 | 2.7 | – | – |
| 6 | 6.7 | – | – |
| 7 | 34 | – | – |
| 8 | 9.8 | ND | – |
| 9 | 11.1 | + | + |
| 10 | 0.6 | – | – |
| 11 | 0.4 | ND | – |
| 12 | 2.3 | – | – |
| T-ALL | 0.16 | – | – |

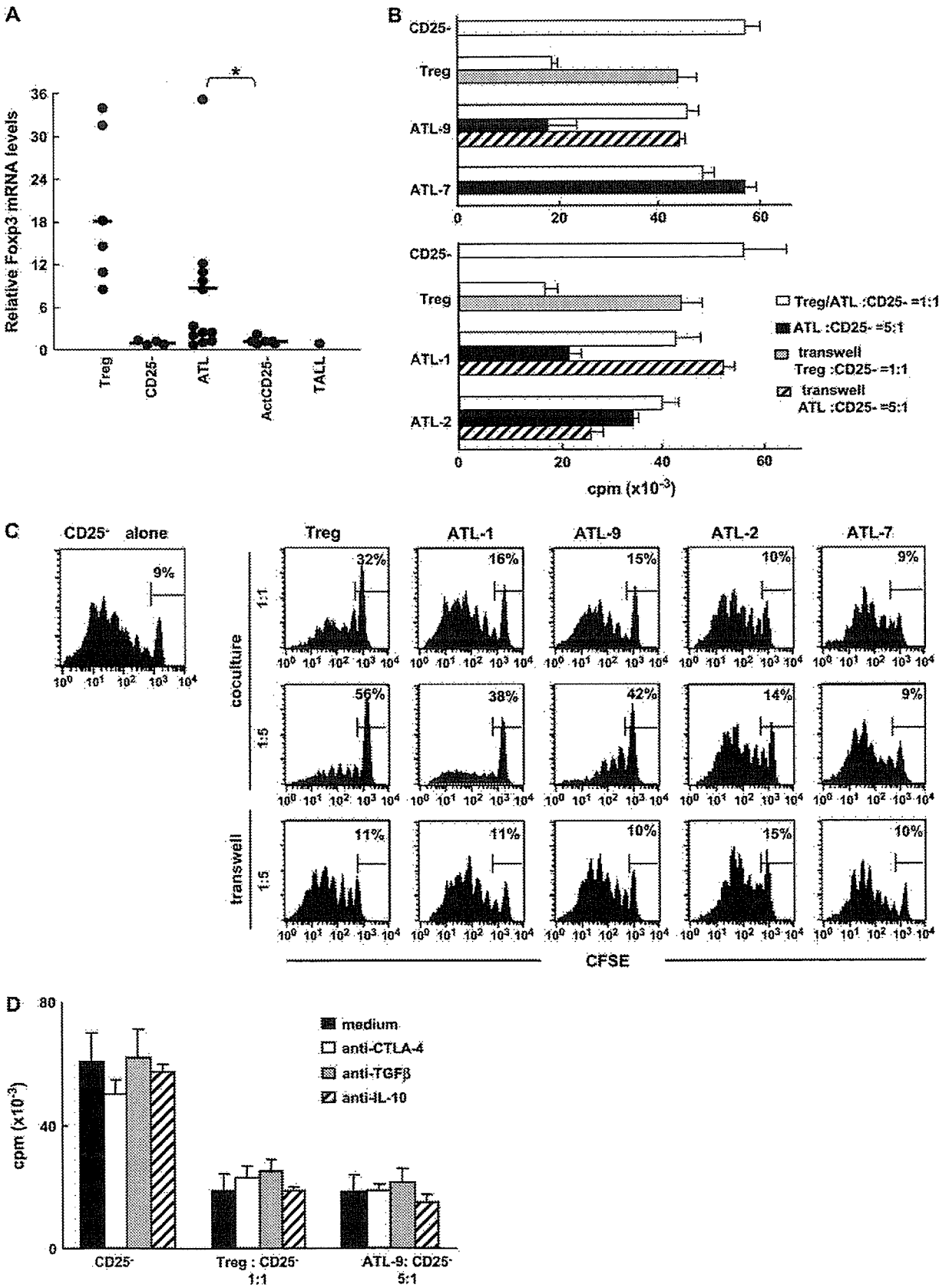
A
Relative Foxp3 mRNA levels
36
30
24
18
12
6
0
*
Treg
CD25-
ATL
ActCD25-
TALL
B
CD25-
Treg
ATL-9
ATL-7
0
20
40
60
CD25-
Treg
ATL-1
ATL-2
0
20
40
60
cpm (x10-3)
Treg/ATL :CD25- =1:1
ATL :CD25- =5:1
transwell
Treg :CD25- =1:1
transwell
ATL :CD25- =5:1
C
CD25- alone
9%
Treg
ATL-1
ATL-9
ATL-2
ATL-7
coculture
1:1
1:5
transwell
1:5
32%
16%
15%
10%
9%
56%
38%
42%
14%
9%
11%
11%
10%
15%
10%
CFSE
D
80
40
0
cpm (x10-3)
medium
anti-CTLA-4
anti-TGFβ
anti-IL-10
CD25-
Treg : CD25-
1:1
ATL-9: CD25-
5:1

the other hand, Treg cells can mediate suppressive activity in a cytokine-independent manner (7). We therefore examined whether a panel of inhibitory cytokines or factors could mediate the ATL-cell-induced suppression. The addition of neutralizing antibodies for CTLA-4, TGFβ or IL-10 to a co-culture of ATL cells from patient 9 with responder T cells did not affect the inhibitory activity of the ATL cells (Fig. 1D). These results indicate that a cytokine-independent mechanism may be responsible for the suppression. Based on the above results, we reasoned that ATL-cell-induced suppression may mimic the cell–cell contact-dependent mechanism by which Treg cells mediate suppression. To test this possibility, we next performed a series of trans-well experiments. Separating ATL cells from the $CD25^-CD4^+$ responder T cells abolished the suppressive activity of the ATL cells from patients 1 and 9 (Fig. 1B and C). Note, however, that the suppression caused by the ATL cells from patient 2 was not fully abrogated by separation from the responder T cells (Fig. 1B and C).

### *Foxp3 expression and the suppressive activity of HTLV-I-infected cell lines*

We also measured the Foxp3 expression in some ATL cell lines (EDγ-16 and TL-Om1) and *in vitro*-established HTLV-I-infected cell lines (MT-2, ILT-Mat, TCL-Mor, TCL-Kan). Except for MT-2, none of these cell lines expressed Foxp3 mRNA (Fig. 2A). We then examined the suppressive activity of these cell lines by co-culturing them with CFSE-labeled $CD25^-CD4^+$ T cells. The cell division profiles of $CD25^-CD4^+$ T cells co-cultured with MT-2 were similar to those obtained with Treg cells (Fig. 2B). In contrast, the TL-Om1 (Fig. 2B and C) cells and other cell lines did not inhibit cell division and cell proliferation (data not shown). Furthermore, to investigate the mechanism for the suppressive activity of MT-2, we performed a trans-well experiment. As we had seen with the Treg cells, the separation of the MT-2 from the $CD25^-CD4^+$ T cells abolished the MT-2-cell-induced suppression of the division of conventional CD4 T cells and restored the CD4 T cell number (Fig. 2B and C). In addition, as with ATL-induced suppression, none of the neutralizing antibodies for CTLA-4, TGFβ or IL-10 changed the inhibitory activity of the MT-2 cells (data not shown).

### *Forced expression of Foxp3 failed to produce suppressive activity in HTLV-I-infected cell lines*

Since the Treg-like ATL cells (from patients 1 and 9) and MT-2 cell lines, all of which expressed high Foxp3 expression, showed regulatory activity, we next addressed the role of Foxp3 in the suppressive function of ATL cells. An ATL cell line (EDγ-16) and an HTLV-I-infected T cell line (ILT-Mat) were transfected with the Foxp3 gene using a retroviral vector (Fig. 3A). Although deliberate Foxp3 expression converts primary conventional CD4 T cells to Treg-like suppressor cells *in vitro* (7), Foxp3 expression in these ATL and HTLV-I-infected cell lines failed to induce any apparent suppressive function (Fig. 3B). These results suggest that Foxp3 expression is not sufficient to elicit the Treg cell function in ATL and HTLV-I-infected cells. This idea is supported by the negligible suppressive activity of the ATL cells from patient 7, even though they expressed the highest Foxp3 level among the ATL cells used in this study (Table 2, Fig. 1B and C).

### *T cell activation could not induce Foxp3 expression*

Several reports suggest that activated T cells that are stimulated under certain conditions acquire Foxp3 expression (21, 22). Others, however, have been unable to reproduce the Foxp3 induction in these activated T cells (23). We therefore examined the Foxp3 induction in primary activated CD4 T cells, which we stimulated in a variety of ways, according to previous reports, and failed to detect any obvious Foxp3 induction in these activated T cells (Fig. 4A), in agreement with Yagi *et al.* (23).

### *HTLV-I Tax expression or HTLV infection failed to induce Foxp3 expression in T cells*

Since the *tax* gene in HTLV-I has been considered an essential transactivator for the tumorigenesis of HTLV-I-infected T cells through its induction of several cellular genes (2), we also examined whether Tax could induce Foxp3 expression. Although *tax* gene induction in a human T cell line, Jurkat, induced the surface expression of OX40L (Fig. 4B), which is a good target for Tax (24, 25), Tax could not induce Foxp3 expression in Jurkat cell lines (Fig. 4C). Finally, to examine

**Fig. 1.** ATL cells are phenotypically and functionally similar to Treg cells. (A) Relative expression of the Foxp3 transcript in ATL cells. Total RNA was isolated from ATL ($n = 12$), Treg ($n = 6$), freshly isolated $CD25^-CD4^+$ T ($n = 4$) and activated $CD25^-CD4^+$ T ($n = 6$) cells by Trizol Reagent (Invitrogen, Carlsbad, CA), and converted to cDNA. Activated T cells were prepared by culturing of $CD25^-CD4^+$ T cells for 2 days in the presence of coated anti-CD3 mAb (5 μg $ml^{-1}$) and soluble anti-CD28 mAb (2 μg $ml^{-1}$). The relative expression of the Foxp3 transcript was estimated by real-time PCR. As an endogenous control, a set of primers and a probe specific for human GAPDH mRNA (Applied Biosystems) was used. In each amplification, the cDNAs were quantified using relative standard curves. All results were normalized with respect to the internal control. The significance of the data was evaluated by Student's *t*-test (* represents $p < 0.05$). (B) Suppressive activity of ATL cells. $CD25^-CD4^+$ T cells ($5 \times 10^4$) were stimulated with anti-CD3 mAb in the presence of DCs. ATL cells or Treg cells and DCs were added at the indicated ratio directly to the culture or were placed in trans-well chambers. [$^3$H]TdR incorporation of cells cultured in the lower well during the last 4 h of a 5-day culture was measured as an indicator of cell proliferation and is expressed as the mean (±SD) of triplicate cultures. This figure shows four representative ATL samples, including suppressive ATL cells from patients 1, 2 and 9, and non-suppressive ATL cells from patient 7. (C) Suppressive activity of ATL cells. Co-culture and trans-well experiments using CFSE-labeled $CD25^-CD4^+$ T cells were performed as described above. The CFSE intensity of $CD25^-CD4^+$ T cells after a 5-day culture was measured with a flow cytometer. The frequency (%) of cells failing to undergo cell division is indicated in the figure. Representative results of the suppressive ATL cells from patients 1, 2 and 9, and non-suppressive ATL cells from patient 7 are shown. (D) The neutralization of regulatory molecules did not affect the ATL-cell-mediated suppression. $CD25^-CD4^+$ T cells ($5 \times 10^4$) were stimulated with anti-CD3 mAb in the presence of Treg cells ($5 \times 10^4$) or ATL cells from patient 9 ($5 \times 10^4$ or $2.5 \times 10^5$). Neutralizing antibodies (10 μg $ml^{-1}$) for CTLA-4, TGFβ or anti-IL-10 were added to the cultures. [$^3$H]TdR incorporation during the last 4 h of a 5-day culture was measured as an indicator of cell proliferation and is expressed as the mean (±SD) of triplicate cultures. Similarly, addition of these neutralizing antibodies did not affect the suppression mediated by ATL cells from patients 1 and 2 (data not shown).

whether HTLV-I infection could induce Foxp3 expression in conventional CD4 T cells, purified $CD25^-CD4^+$ T cells were infected with HTLV-I. Figure 4(D) shows that HTLV-I infection did not change the Foxp3 expression in two independent $CD25^-CD4^+$ T cell clones. These results suggest that HTLV-I infection may not be associated with high Foxp3 expression in ATL cells.

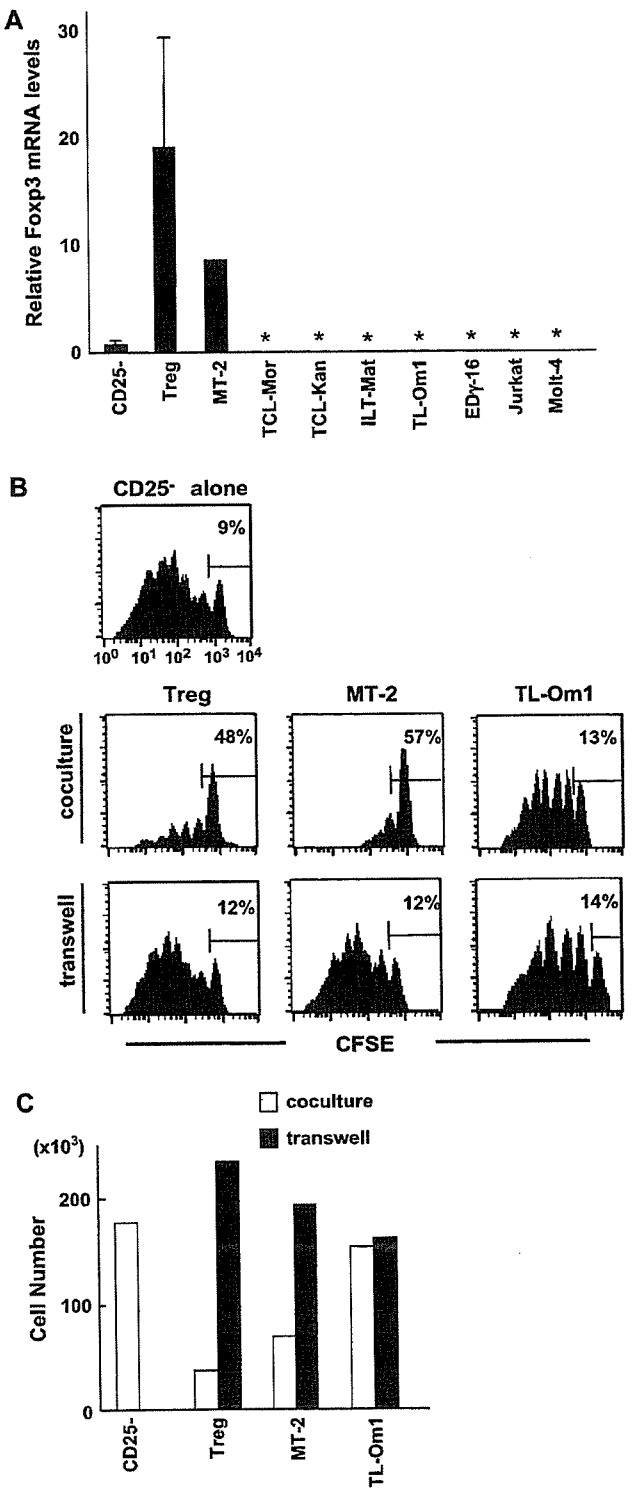


## Discussion

In the present study we detected high Foxp3 expression, which is a good marker for $CD25^+CD4^+$ Treg cells, in 5 of 12 ATL cell isolates (Table 2). In addition, two of the five Foxp3-expressing ATL cell isolates possessed Treg-like characteristics, not only in having high Foxp3 expression but also in having a suppressive function on $CD25^-CD4^+$ T cells that is mediated by cell–cell contact (Fig. 1B and C). Although four recent papers have reported Foxp3 expression in ATL cells (10–13), here we show the first evidence that ATL cells have a Treg-like regulatory function. Furthermore, MT-2 cells, which express Foxp3 at high levels, also exhibited Treg-like suppressive activity. These results indicate that some ATL cells have an immunosuppressive activity resembling that of Treg cells. Considering that cellular immunodeficiency is observed in a quarter of patients with ATL (2–4), we hypothesize that immunosuppressive activity by ATL cells may contribute to the immunodeficiency. The immunodeficiency-associated infection seen in two patients (patients 1 and 2) (Table 1), whose cells were suppressive, may support this idea, although the suppressive mechanism of the ATL cells from patient 2 might be different from that of Treg cells. Although it may seem at first glance that our experimental system is artificial because it used four times more ATL cells than Treg cells to show the suppressive activity, many patients have a large number of ATL cells, which could be sufficient to provide the suppressive activity *in vivo*. As shown in Table 1, leukemia cells account for ~90% of the PBMCs in most patients with ATL, in contrast to the much lower population (1–2% of PBMCs) of primary Treg cells in healthy donors. Thus, when the ATL cells have Treg-like suppressive effects, they may contribute to the immunosuppression in patients with ATL, because of their high population in PBMCs.

In both humans and mice, the retroviral gene transfer of Foxp3 converts conventional CD4 T cells ($CD25^-CD4^+$ T cells) to Treg-like suppressor cells (23, 26). Thus, Foxp3 expression has been thought to be essential and sufficient for Treg cell function (7). In our study, two ATL cells (from patients 1 and 9) and one HTLV-I-infected cell line (MT-2), all of which showed high Foxp3 expression, had Treg-like suppressive activity that is mediated by a cell–cell contact mechanism (Fig. 1B and C). In contrast, ATL cells (from patient 2) with a lower level of

**Fig. 2.** Foxp3 expression and suppressive activity of HTLV-I-infected cell lines. (A) Foxp3 expression in ATL, HTLV-I-infected, and non-infected T cell lines. Foxp3 expression in T cell lines was determined by real-time PCR as described in Fig. 1A. The mRNA expression of Foxp3 was normalized to the copies of GAPDH mRNA from the same sample. Asterisks represent undetectable levels of the Foxp3 transcript. (B) Suppressive activity of HTLV-I-infected cell lines. CFSE-labeled $CD25^-CD4^+$ T cells ($5 \times 10^4$) were stimulated with soluble anti-CD3 mAb in the presence of irradiated DCs. Treg cells, MT-2 cells or TL-Om1 cells ($2.5 \times 10^4$ each) were added directly to the cultures or placed into trans-well chambers. After 5 days of culture, the CFSE intensity was measured by FACS as an indicator of cell division. The frequency (%) of cells failing to undergo cell division is indicated in the figure. (C) Trans-well separation abrogates the MT-2-cell-associated suppression of CD4 T cell proliferation. The same experiments were performed as described in (B). The number of live CFSE-labeled $CD4^+$ T cells was counted 5 days after CD3 stimulation. Similar results were obtained in three independent experiments.

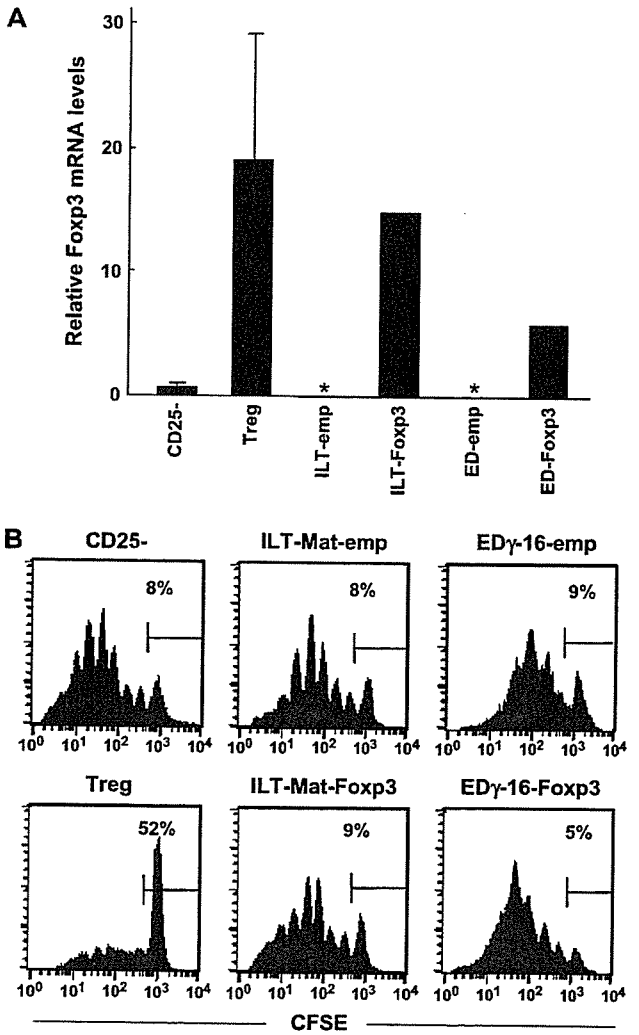


**Fig. 3.** Forced expression of Foxp3 cannot convert HTLV-I-infected cells to Treg-like suppressive cells. (A) Foxp3 expression in HTLV-I-infected cell lines transfected with the Foxp3 gene. Foxp3 expression in Foxp3-transfected ILT-Mat and EDγ-16 cells was determined in comparison with that in empty-vector-transfected cells by real-time PCR, as described in Fig. 1A. The mRNA expression of Foxp3 was normalized to the copies of GAPDH mRNA from the same sample. Asterisks represent undetectable levels of the Foxp3 transcript. (B) Suppressive activity of Foxp3-transfected cell lines. Co-culture of CFSE-labeled $CD25^{-}CD4^{+}$ T cells ($5 \times 10^4$) with the Foxp3-transfected cell lines ($2.5 \times 10^4$) was performed as described in Fig. 2(B). After 5 days of culture, the CFSE intensity was measured by FACS, as an indicator of cell division. The frequency of cells failing to undergo cell division is indicated in the figure.

Foxp3 expression were able to suppress T cell responses even in the presence of a transmembrane (Fig. 1B and C). While a close association between Foxp3 expression and Treg-like suppressive activity can be inferred from this result, it is clear nevertheless that ATL cells derived from patient 2 may harbor an alterative mechanism of suppression. To directly address the functional association between Foxp3 expression and suppressive activity of ATL cells, deliberate suppression of Foxp3 expression in ATL cells such as the use of siRNAs may be required. However, this may be challenging as freshly isolated ATL cells do not proliferate *in vitro* and are therefore resistant to any gene-transfer treatment. In addition, to our knowledge, no study has demonstrated that deliberate knock-down of Foxp3 expression in Treg cells abrogates their suppressive activity. A recent report by Sereti *et al.* shows that overexpression of two Foxp3 isoforms on $CD25^{-}CD4^{+}$ T cells, could induce the generation of phenotypic Treg cells but with poor suppressive activity (27). Thus, functional roles of Foxp3 expression for Treg-like suppression by not only ATL cells but also by Treg cell remain completely unresolved.

Some of the ATL cells (from patients 6 and 7), in spite of their high Foxp3 expression, did not show any inhibitory activity. In addition, the forced expression of Foxp3 in non-Foxp3-expressing T cell lines could not confer the suppressive activity (Fig. 3B). These results indicate that Foxp3 is not sufficient for the suppressive activity of ATL cells, ATL cell lines and HTLV-I-infected cell lines. Other factor(s) in addition to Foxp3 may be essential for the suppressive function. During a long neoplastic process, such factor(s) might be lost by the ATL cells, rendering them non-suppressive in spite of their high Foxp3 expression.

With regard to the origin of ATL cells, we speculate that there might be at least two distinct subsets of $CD25^{+}$ ATL cells in terms of Foxp3 expression. The ones with Treg-like features may be derived from primary Foxp3-expressing cells, because HTLV-I infection, Tax induction and other mitogenic stimulations of T cells could not induce Foxp3 expression in our system. Furthermore, Tax expression does not correlate with Foxp3 expression in ATL cells (Table 2). In contrast, the leukemia cells from some patients with ATL (patients 4, 10 and 11) showed a low level of Foxp3 and negligible regulatory activity, which resemble the characteristics of activated T cells. In addition, the TL-Om1 and EDγ-16 cell lines, which were derived from ATL cells, demonstrated neither high Foxp3 expression nor the suppressive function. Thus, another subset of ATL cells may be derived from activated T cells, as previously thought. An interesting question is whether the origins of ATL cells can be classified into two different T cell types, activated T and Treg cells. The analysis of *in vitro*-established HTLV-I-infected cell lines can help us explore the origin of ATL cells. Most of the HTLV-I-infected cell lines were established by using whole peripheral T cells, including both Treg and non-Treg T cells, as the infection targets, which is closer to the physiological condition than the use of an isolated cell population. Among the six HTLV-I-infected cell lines we checked, MT-2 cells expressed Foxp3 and harbored the Treg-cell-like function, suggesting that MT-2 cells may have originated from Treg cells. Our preliminary results demonstrated that HTLV-I could infect purified $CD25^{+}CD4^{+}$ T cells and that the HTLV-I-infected Treg cells still showed high Foxp3 expression (data not shown). In contrast, HTLV-I infection failed to induce Foxp3 expression in purified $CD25^{-}CD4^{+}$ T cells (Fig. 4D). These results support the idea that ATL and HTLV-I-infected cell lines that sustain high Foxp3 expression may be derived from Treg cells. Since Treg cells are anergic to stimulation with antigen, HTLV-I, which is a typical retrovirus, may selectively infect proliferating conventional CD4 T cells *in vitro*. This is the likely reason so few HTLV-I-infected Treg cell lines were obtained. To investigate properly the leukemogenesis of Treg cells as the origin of ATL cells, appropriate

methods for the HTLV-I infection of Treg cells may be essential, although it may be difficult to render Treg cells susceptible to HTLV-I retrovirus by inducing cell division. Nevertheless, further studies on the cellular origins of ATL cells will improve our understanding of how ATL and its associated immunosuppression develop in human patients.

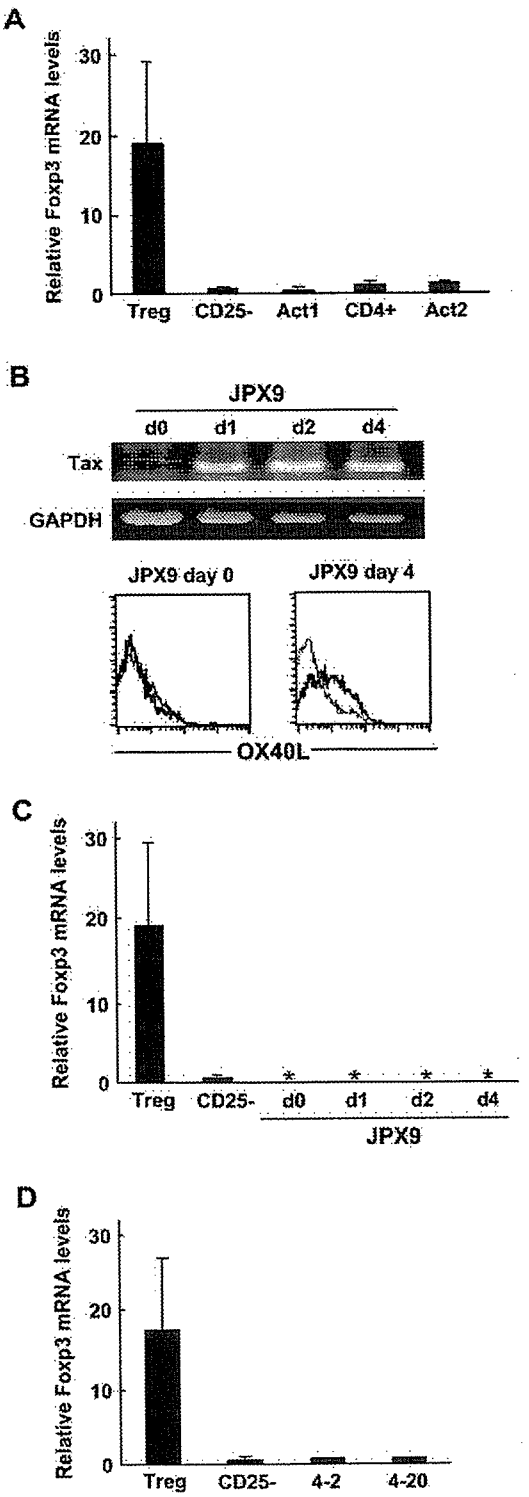


## Acknowledgements

This work was supported in part by a grant-in-aid for scientific research on priority areas from the Ministry of Education, Culture, Sports, Science and Technology of Japan, and a grant-in-aid for scientific research on priority areas from the Japan Society for the Promotion of Science.

## Abbreviations

| | |
|---|---|
| ATL | adult T cell leukemia |
| HTLV-I | human T cell leukemia virus type I |
| DC | dendritic cell |
| Treg | regulatory T cells |
| CTLA-4 | cytotoxic T lymphocyte antigen 4 |
| CFSE | 5,6-carboxy-fluorescein succinimidyl ester |

## References

1 Hinuma, Y., Nagata, K., Hanaoka, M. *et al.* 1981. Adult T-cell leukemia: antigen in an ATL cell line and detection of antibodies to the antigen in human sera. *Proc. Natl. Acad. Sci. USA* 78:6476.
2 Uchiyama, T. 1997. Human T cell leukemia virus type I (HTLV-I) and human diseases. *Annu. Rev. Immunol.* 15:15.
3 Shimoyama, M. 1991. Diagnostic criteria and classification of clinical subtypes of adult T-cell leukaemia-lymphoma. A report from the Lymphoma Study Group (1984-87). *Br. J. Haematol.* 79:428.
4 Matsuoka, M. 2003. Human T-cell leukemia virus type I and adult T-cell leukemia. *Oncogene* 22:5131.
5 Yasunaga, J., Sakai, T., Nosaka, K. *et al.* 2001. Impaired production of naive T lymphocytes in human T-cell leukemia virus type I-infected individuals: its implications in the immunodeficient state. *Blood* 97:3177.
6 Sugamura, K., Fujii, M., Kannagi, M., Sakitani, M., Takeuchi, M. and Hinuma, Y. 1984. Cell surface phenotypes and expression of viral antigens of various human cell lines carrying human T-cell leukemia virus. *Int. J. Cancer* 34:221.
7 Sakaguchi, S. 2004. Naturally arising CD4+ regulatory t cells for immunologic self-tolerance and negative control of immune responses. *Annu. Rev. Immunol.* 22:531.
8 Shevach, E. M. 2002. CD4+ CD25+ suppressor T cells: more questions than answers. *Nat. Rev. Immunol.* 2:389.

**Fig. 4.** Foxp3 expression was not induced during T cell activation or HTLV-I infection. (A) Foxp3 expression was not be induced in activated T cells. Several recent reports demonstrated that certain procedures for T cell activation can induce Foxp3 expression. Therefore, according to the methods described in these papers, $CD25^{-}CD4^{+}$ T cells were activated with coated anti-CD3 and soluble anti-CD28 for 1 day and then cultured in the absence of stimulants for three more days (Act1) (21). Alternatively, $CD4^{+}$ T cells were stimulated with allogeneic APCs in the presence of IL-2 and TGFβ for 6 days (Act2) (23). Foxp3 expression in Treg cells and activated $CD4^{+}$ T cells before ($CD25^{-}$ or $CD4^{+}$) and after stimulation (Act 1–2) was measured by real-time PCR as described in Fig. 1A. (B) Tax induction in Jurkat cells. JPX9 cells were treated with 30 μM $CdCl_2$. Tax expression and induction of OX40L, a target for tax, were confirmed at the indicated days after treatment. Thick and thin lines in the lower panels represent OX40L staining and control staining, respectively. (C) HTLV-I tax induction did not affect the Foxp3 expression in Jurkat cells. JPX9 cells were collected at the indicated days after stimulation, and their Foxp3 expression was measured by real-time PCR, as described above. Asterisks represent undetectable levels of the Foxp3 transcript. (D) HTLV-I infection of $CD25^{-}CD4^{+}$ T cells does not change their Foxp3 expression. The Foxp3 expression in freshly isolated $CD25^{-}CD4^{+}$ T cells and two independent HTLV-infected cell clones (4-2 and 4-20) that were established from purified $CD25^{-}CD4^{+}$ T cells by co-culture with MT-2 cells was estimated by real-time PCR, as described above.

9 Ndhlovu, L. C., Takeda, I., Sugamura, K. and Ishii, N. 2004. Expanding role of T-cell costimulators in regulatory T-cell function: recent advances in accessory molecules expressed on both regulatory and nonregulatory T cells. *Crit. Rev. Immunol.* 24:251.
10 Karube, K., Ohshima, K., Tsuchiya, T. *et al.* 2004. Expression of FoxP3, a key molecule in CD4CD25 regulatory T cells, in adult T-cell leukaemia/lymphoma cells. *Br. J. Haematol.* 126:81.
11 Ishida, T., Iida, S., Akatsuka, Y. *et al.* 2004. The CC chemokine receptor 4 as a novel specific molecular target for immunotherapy in adult T-cell leukemia/lymphoma. *Clin. Cancer Res.* 10:7529.
12 Matsubara, Y., Hori, T., Morita, R., Sakaguchi, S. and Uchiyama, T. 2005. Phenotypic and functional relationship between adult T-cell leukemia cells and regulatory T cells. *Leukemia* 19:482.
13 Kohno, T., Yamada, Y., Akamatsu, N. *et al.* 2005. Possible origin of adult T-cell leukemia/lymphoma cells from human T lymphotropic virus type-1-infected regulatory T cells. *Cancer Sci.* 96:527.
14 Sugamura, K., Nakai, S., Fujii, M. and Hinuma, Y. 1985. Interleukin 2 inhibits in vitro growth of human T cell lines carrying retrovirus. *J. Exp. Med.* 161:1243.
15 Miyoshi, I., Kubonishi, I., Yoshimoto, S. and Shiraishi, Y. 1981. A T-cell line derived from normal human cord leukocytes by co-culturing with human leukemic T-cells. *Gann* 72:978.
16 Maeda, M., Shimizu, A., Ikuta, K. *et al.* 1985. Origin of human T-lymphotrophic virus I-positive T cell lines in adult T cell leukemia. Analysis of T cell receptor gene rearrangement. *J. Exp. Med.* 162:2169.
17 Ishii, N., Asao, H., Kimura, Y. *et al.* 1994. Impairment of ligand binding and growth signaling of mutant IL-2 receptor gamma-chains in patients with X-linked severe combined immunodeficiency. *J. Immunol.* 153:1310.
18 Nagata, K., Ohtani, K., Nakamura, M. and Sugamura, K. 1989. Activation of endogenous c-fos proto-oncogene expression by human T-cell leukemia virus type I-encoded p40tax protein in the human T-cell line, Jurkat. *J. Virol.* 63:3220.
19 Mori, N., Gill, P. S., Mougdil, T., Murakami, S., Eto, S. and Prager, D. 1996. Interleukin-10 gene expression in adult T-cell leukemia. *Blood* 88:1035.
20 Niitsu, Y., Urushizaki, Y., Koshida, Y. *et al.* 1988. Expression of TGF-beta gene in adult T cell leukemia. *Blood* 71:263.
21 Walker, M. R., Kasprowicz, D. J., Gersuk, V. H. *et al.* 2003. Induction of FoxP3 and acquisition of T regulatory activity by stimulated human CD4+CD25− T cells. *J. Clin. Invest.* 112: 1437.
22 Zheng, S. G., Wang, J. H., Gray, J. D., Soucier, H. and Horwitz, D. A. 2004. Natural and induced CD4+CD25+ cells educate CD4+CD25− cells to develop suppressive activity: the role of IL-2, TGF-beta, and IL-10. *J. Immunol.* 172:5213.
23 Yagi, H., Nomura, T., Nakamura, K. *et al.* 2004. Crucial role of FOXP3 in the development and function of human CD25+CD4+ regulatory T cells. *Int. Immunol.* 16:1643.
24 Miura, S., Ohtani, K., Numata, N. *et al.* 1991. Molecular cloning and characterization of a novel glycoprotein, gp34, that is specifically induced by the human T-cell leukemia virus type I transactivator p40tax. *Mol. Cell. Biol.* 11:1313.
25 Higashimura, N., Takasawa, N., Tanaka, Y., Nakamura, M. and Sugamura, K. 1996. Induction of OX40, a receptor of gp34, on T cells by trans-acting transcriptional activator, Tax, of human T-cell leukemia virus type I. *Jpn. J. Cancer Res.* 87:227.
26 Hori, S., Nomura, T. and Sakaguchi, S. 2003. Control of regulatory T cell development by the transcription factor Foxp3. *Science* 299:1057.
27 Allan, S. E., Passerini, L., Bacchetta, R., Crellin, N., Dai, M., Orban, P. C., Ziegler, S. F., Roncarolo, M. G., and Levings, M. K. 2005. The role of 2 FOXP3 isoforms in the generation of human CD4+ Tregs. *J. Clin. Invest.* 115:3276.

THE JOURNAL OF GENE MEDICINE
*J Gene Med* 2006; **8**: 646–653.
Published online 28 February 2006 in Wiley InterScience (www.interscience.wiley.com). **DOI:** 10.1002/jgm.891

RESEARCH ARTICLE

# Phage $\phi$C31 integrase-mediated genomic integration of the common cytokine receptor gamma chain in human T-cell lines

Yoshinori Ishikawa[1]
Nobuyuki Tanaka[1]*
Kazuhiro Murakami[2]
Toru Uchiyama[3]
Satoru Kumaki[3]
Shigeru Tsuchiya[3]
Hiroyuki Kugoh[2]
Mitsuo Oshimura[2]
Michele P. Calos[4]
Kazuo Sugamura[1]

[1]*Department of Microbiology and Immunology, Tohoku University Graduate School of Medicine, 2-1 Seiryo-machi, Aoba-ku, Sendai 980-8575, Japan*

[2]*Department of Biomedical Science, Graduate School of Medical Science, Tottori University, 86 Nishimachi, Yonago 683-8503, Japan*

[3]*Department of Pediatric Oncology, Institute of Development, Aging and Cancer, Tohoku University, 4-1 Seiryo-machi, Aoba-ku, Sendai 980-8575, Japan*

[4]*Department of Genetics, Stanford University School of Medicine, Stanford, CA 94305-5120, USA*

*Correspondence to:
Nobuyuki Tanaka, Department of Microbiology and Immunology, Tohoku University Graduate School of Medicine, 2-1 Seiryo-machi, Aoba-ku, Sendai 980-8575, Japan.
E-mail:
n-tanaka@mail.tains.tohoku.ac.jp

*Received: 19 October 2005*
*Revised: 27 December 2005*
*Accepted: 28 December 2005*

## Abstract

**Background** X-linked severe combined immunodeficiency (SCID-X1, X-SCID) is a life-threatening disease caused by a mutated common cytokine receptor $\gamma$ chain ($\gamma$c) gene. Although *ex vivo* gene therapy, i.e., transduction of the $\gamma$c gene into autologous CD34$^+$ cells, has been successful for treating SCID-X1, the retrovirus vector-mediated transfer allowed dysregulated integration, causing leukemias. Here, to explore an alternative gene transfer methodology that may offer less risk of insertional mutagenesis, we employed the $\phi$C31 integrase-based integration system using human T-cell lines, including the $\gamma$c-deficient ED40515(-).

**Methods** A $\phi$C31 integrase and a *neo*$^r$ gene expression plasmid containing the $\phi$C31 *attB* sequence were co-delivered by electroporation into Jurkat cells. After G418 selection, integration site analyses were performed using linear amplification mediated-polymerase chain reaction (LAM-PCR). ED40515(-) cells were also transfected with a $\gamma$c expression plasmid containing *attB*, and the integration sites were determined. IL-2 stimulation was used to assess the functionality of the transduced $\gamma$c in an ED40515(-)-derived clone.

**Results** Following co-introduction of the $\phi$C31 integrase expression plasmid and the plasmid carrying *attB*, the efficiency of integration into the unmodified human genome was assessed. Several integration sites were characterized, including new integration sites in intergenic regions on chromosomes 13 and 18 that may be preferred in hematopoietic cells. An ED40515(-) line bearing the integrated $\gamma$c gene exhibited stable expression of the $\gamma$c protein, with normal IL-2 signaling, as assessed by STAT5 activation.

**Conclusions** This study supports the possible future use of this $\phi$C31 integrase-mediated genomic integration strategy as an alternative gene therapy approach for treating SCID-X1. Copyright © 2006 John Wiley & Sons, Ltd.

**Keywords** site-specific integration; $\phi$C31 integrase; SCID-X1; hematopoietic cells

## Introduction

X-linked severe combined immunodeficiency (SCID-X1) is the most frequent form of severe combined immunodeficiency (SCID) [1,2]. A number of studies have demonstrated that mutations within the common cytokine receptor $\gamma$ chain ($\gamma$c) gene cause this life-threatening disease. As a shared receptor

Copyright © 2006 John Wiley & Sons, Ltd.

component of multiple cytokine receptors, including the interleukin-2 (IL-2), IL-4, IL-7, IL-9, IL-15, and IL-21 receptors, the $\gamma$c protein is required for the normal development of hematopoietic cell populations, including T and NK cells, as well as the normal function of B cells, in humans. Dysfunction of the $\gamma$c, therefore, causes the SCID-X1 phenotypes. Because there is a single causative gene for this lethal disease, patients can be cured by transfusion with a population of their own $CD34^+$ bone marrow cells transfected *ex vivo* with the normal $\gamma$c gene [3,4]. Indeed, a clinical trial using retroviral transfer of the $\gamma$c cDNA into hematopoietic stem cells (HSC) successfully reconstituted the hematopoietic cell populations of the affected patients [5–7]. Unexpectedly, however, almost 3 years following the initial therapy, three of the ten SCID patients developed severe adverse effects, such as leukemia [8,9]. In at least two cases, the same proto-oncogene, LMO-2, was transcriptionally activated, due to integration of the retroviral vector near the LMO-2 promoter [10]. To reduce the risk of such insertional activation of cellular proto-oncogenes, alternative safer gene delivery/integration methods are desirable [11].

Bacteriophage integrases are enzymes that mediate site-specific recombination between two DNA recognition sequences [12]. Among such integrases, $\phi$C31 integrase, which has a catalytic serine residue and is therefore classified as a member of the serine integrase family, mediates specific recombination between the phage attachment site *attP* and the bacterial attachment site *attB*. $\phi$C31 integrase mediates the integration of plasmids bearing an *attB* site into a limited number of 'pseudo-*attP*' sites present in native mammalian genomes. Given that $\phi$C31 integrase recognizes relatively short, yet still rather specific, sequences in mammalian genomes, it is becoming a promising genetic manipulation tool in eukaryotes [13,14]. Indeed, by using this strategy, enzyme genes have been stably integrated into the livers of mice after high-pressure tail vein injection, resulting in the prolonged expression of therapeutic genes [15,16]. The $\phi$C31 integrase system has also been applied to the *ex vivo* modification of human primary skin and muscle progenitor cells for autotransplantation [17,18].

Because HSC can be manipulated *ex vivo*, SCID-X1 may be a feasible candidate for $\phi$C31 integrase-mediated gene therapy. In this study, we demonstrate that the $\phi$C31 integrase functions in human T-cell lines. We also identify pseudo-*attP* sites into which the therapeutic gene integrates and assess the feasibility of this strategy for SCID-X1 gene therapy by demonstrating the correction of a $\gamma$c-deficient human T-cell line.

# Materials and methods

## Plasmid construction

pCMVInt was used for $\phi$C31 integrase expression [12]. A carrier plasmid pCS was generated by removing the integrase gene from pCMVInt using *BamHI-SpeI* followed by blunt-end ligation. The *attB* sequence-containing plasmids, pcDNA-attB and pCXB, were constructed as follows: the *EcoRI* fragment containing the $\phi$C31 *attB* sequence from pTA-attB [12] was blunt-ligated into the *BglII* site of the backbone vector pcDNA3 and the *HindIII* site of pCXN2 [19]. A 1.7-kb *HindIII-XbaI* fragment containing the firefly luciferase gene was excised from the pGL3-promoter (Promega, Madison, WI, USA), the ends were blunted, and the fragment was subcloned into pCXN2 or pCX-B at a blunted *EcoRI* site, generating pCXL and pCXLB, respectively. The human $\gamma$c gene was removed from pSRG1 [20] by digestion with *XbaI* and inserted into *EcoRI* site of pCXB, generating pCX$\gamma$B. Plasmid constructs were verified by DNA sequencing of their respective inserts.

## Cell culture and transfection

An HTLV-transformed human T-cell line, ED40515(-), lacks expression of the $\gamma$c [21]. Jurkat and ED40515(-) cells were maintained in RPMI 1640 supplemented with 10% fetal calf serum and antibiotics. Jurkat cells ($1 \times 10^7$) were transformed by electroporation with 10 μg pcDNA-attB and 10 μg pCMVInt, using pulses of 270 V, 960 μF from a Gene Pulser II (Bio-Rad, Hercules, CA, USA). The electroporation conditions for ED40515(-) were pulses of 350 kV at 250 μF. Cells were split into a 96-well plate at the appropriate dilution. One day after transfection, G418-containing medium was added to a final concentration of 600 μg/ml, and the cells were cultured for at least 3 more weeks.

## Luciferase assay

Jurkat cells were seeded in 24-well plates at a density of $1 \times 10^5$ cells per ml, 36 h before they were transfected with 1.5 μg of either pCXL or pCXLB and 1.5 μg of either carrier plasmid pCS or pCMVInt, using 4 μl of DIMRIE-C (Invitrogen, Carlsbad, CA, USA). Twenty-four hours after transfection, the cells were transferred into flasks with 6 ml of medium. Seventy-two hours after the transfection, 80% of the cells were harvested for use in the assays. The remaining cells were further cultured with a maintenance medium exchange every 3 days. Luciferase assays were performed using a luciferase assay system (Promega) according to the manufacturer's instructions.

## Linear amplification mediated-polymerase chain reaction (LAM-PCR)

LAM-PCR was performed using the previously reported methodology with slight modifications [22]. Briefly, genomic DNA from transfectant clones passaged at least 3 weeks was purified using the GenElute mammalian genomic DNA Miniprep kit (Sigma, St.Louis, MO, USA), and used as the template. Linear amplification was carried out with the biotinylated primer B1 (5′-ctg acg ctg ccc cgc

Copyright © 2006 John Wiley & Sons, Ltd.

gta tcc gca c-3′). Biotinylated products were selected with streptavidin magnetic beads (Dynal, Oslo, Norway). Random priming was performed with random hexamers (Roche, Indianapolis, IN, USA) and the Klenow fragment. The products were digested by *Tsp*501I and then ligated into a linker cassette, which was generated by annealing two oligonucleotides: 5′-gac ccg gga gat ctg aat tca gtg gca cag cag tta gg-3′ and 5′-aat tcc taa ctg ctg tgc cac tga att cag atc tcc cgg gtc-3′. The resultant ligated products were exponentially amplified twice using the following primers: B2 (5′-tcc cgt gct cac cgt gac ca-3′) and LC1 (5′-gac ccg gga gat ctg aat tc-3′) for the first PCR; B3 (5′-cca gcg gtt tcg agg gcg ag-3′) and LC2 (5′-gat ctg aat tca gtg gca cag-3′) for the second PCR. The PCR products were separated on a 2% agarose gel. Individual bands were excised and used as the template for the final amplification with primers B4 (5′-ttc gcc ggg atc aac tac-3′) and LC3 (5′-agt ggc aca gca gtt agg-3′). Specific PCR bands were excised and purified with a gel extraction kit (Qiagen GmbH, Hilden, Germany). All PCRs were performed using a Takara PCR thermal cycler Dice (Takara Bio. Inc., Otsu, Japan).

## Sequence analysis

The cycle sequencing of the specific LAM-PCR amplicon was performed using an ABI Prism genetic analyzer 3100 (Applied Biosystems, FosterCity, CA, USA), according to the manufacturer's instructions. The obtained sequence data were analyzed and mapped to the appropriate human chromosome localizations by National Center for Biotechnology Information (NCBI) blast search. Tumor genes were further screened using the tumor gene database (http://condor.bcm.tmc.edu/oncogene.html).

## Fluorescence *in situ* hybridization (FISH) analysis

G418-resistant JD1 was subjected to FISH analyses performed as described previously [23]. A probe for the FISH analyses was prepared from the integrated vector, pcDNA-attB.

## Flow cytometric analysis and immunoblotting

Parental ED40515(-) and G418-resistant ED$\gamma$i6 cells were labeled with either the anti-human $\gamma$c mAb (TUGh4), or its isotype-control antibody. Cell analysis was performed on a FACSCalibur (Becton Dickinson, San Jose, CA, USA) with CellQuest software. Before the immunoblotting, the cells were incubated for 5 min in the presence or absence of 10 nM IL-2 (Ajinomoto Ltd., Tokyo, Japan). Cell lysates were prepared as described previously [24] and separated by sodium dodecyl sulfate-polyacrylamide gel electrophoresis (SDS-PAGE). Western blot analysis was performed with an anti-phospho-STAT5 antibody (Cell Signaling, Beverly, MA, USA). After being stripped of the antibodies, the membrane was further used to monitor the amount of STAT5 protein with specific antisera (Santa Cruz Biotechnology, Santa Cruz, CA, USA).

# Results

To examine whether the $\phi$C31 integrase-mediated gene delivery system functioned in human hematopoietic cells, we first assessed integration efficiency in the Jurkat human T-cell line. Since $\phi$C31 integrase mediates integration into the genome in combination with a donor plasmid containing the *attB* sequence, we constructed a luciferase expression vector with or without the *attB* sequence to investigate their synergistic effect (Figure 1A). Jurkat cells were transfected with either

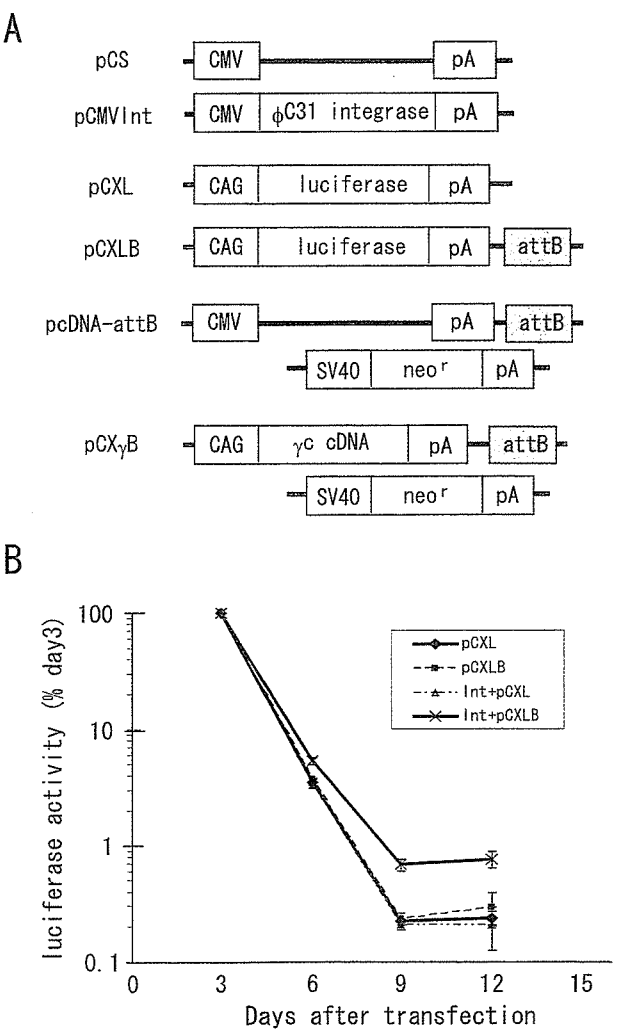


**Figure 1. (A) Schematic map of plasmid constructs used in this study. pCMVInt expresses the $\phi$C31 integrase driven by the CMV promoter. The pCXLB contains the *attB* sequence and a luciferase gene driven by the chicken $\beta$-actin promoter (CAG), and was used to monitor the luciferase activity. (B) The $\phi$C31 integrase/*attB* system mediates persistent luciferase expression in Jurkat cells. Jurkat cells were transfected with the indicated combination of plasmids. The luciferase assay was carried out every 3 days. The relative luciferase activity (%) was calculated after normalization to the initial values from the samples taken 72 h post-transfection**

Copyright © 2006 John Wiley & Sons, Ltd.